

DFTT 43/96
 NORDITA 96/66P
 October 1996

Finite Temperature Lattice QCD in the Large N Limit

M. Billó*

Nordita, Blegdamsvej 17, Copenhagen Ø, Denmark

M. Caselle†, A. D’Adda

*Istituto Nazionale di Fisica Nucleare, Sezione di Torino
 Dipartimento di Fisica Teorica dell’Università di Torino
 via P. Giuria 1, I-10125 Turin, Italy*

S. Panzeri‡

SISSA, Via Beirut 2-4, I-34013, Trieste, Italy

Abstract

Our aim is to give a self-contained review of recent advances in the analytic description of the deconfinement transition and determination of the deconfinement temperature in lattice QCD at large N . We also include some new results, as for instance in the comparison of the analytic results with Montecarlo simulations. We first review the general set-up of finite temperature lattice gauge theories, using asymmetric lattices, and develop a consistent perturbative expansion in the coupling β_s of the space-like plaquettes. We study in detail the effective models for the Polyakov loop obtained, in the zeroth order approximation in β_s , both from the Wilson action (symmetric lattice) and from the heat kernel action (completely asymmetric lattice). The distinctive feature of the heat kernel model is its relation with two-dimensional QCD on a cylinder; the Wilson model, on the other hand, can be exactly reduced to a twisted one-plaquette model via a procedure of the Eguchi–Kawai type. In the weak coupling regime both models can be related to exactly solvable Kazakov–Migdal matrix models. The instability of the weak coupling solution is due in both cases to a condensation of instantons; in the heat kernel case, this is directly related to the Douglas–Kazakov transition of QCD2. A detailed analysis of these results provides rather accurate predictions of the deconfinement temperature. In spite of the zeroth order approximation they are in good agreement with the Montecarlo simulations in $2 + 1$ dimensions, while in $3 + 1$ dimensions they only agree with the Montecarlo results away from the continuum limit.

*E-mail: billlo@alf.nbi.dk; supported by I.N.F.N., Italy

†E-mail: caselle@to.infn.it

‡Present address: *Department of Experimental Psychology, University of Oxford, Oxford OX1 3UD, UK.* E-mail: stefano.panzeri@psy.ox.ac.uk

Contents

1	Introduction	4
2	General Setting	6
2.1	Asymmetric Lattices	6
2.2	Center symmetry and the Polyakov loop	8
2.3	Svetitsky–Yaffe conjecture	9
2.4	\mathbf{Z}_N versus $SU(N)$	11
2.5	Character expansion in the large N limit	13
2.6	Scaling behaviour	15
2.6.1	$d=2$	16
2.6.2	$d=3$	16
3	Construction of the Effective Action	17
3.1	Naive dimensional reduction ($\beta_s = 0$) and related effective actions.	19
3.1.1	$\rho \rightarrow \infty$ limit: heat kernel action	20
3.1.2	Symmetric lattice: Wilson action	21
3.1.3	Scaling behaviours	21
3.1.4	A simplified effective action	23
3.2	Toward an exact dimensional reduction	24
3.2.1	Higher orders in β_s	24
3.2.2	Eguchi–Kawai approach	26
4	Phase diagram of the Effective Model	28
4.1	Weak coupling expansion	29
4.1.1	Solution via the Kazakov–Migdal model	31
4.1.2	Douglas–Kazakov phase transition on a cylinder	33
4.2	Strong coupling expansion	38
4.2.1	Notations and preliminaries	38
4.2.2	The integration measure	40
4.2.3	The kernel on the cylinder	40
4.2.4	The deconfinement transition	42
4.2.5	Instability of the symmetric vacuum	44
5	Extended phase diagrams	47
5.1	Phase diagram in the (J, d) plane	48
5.2	Phase diagram in presence of adjoint quarks	48
5.3	Phase diagram in presence of a “magnetic field”	51
6	Results in the framework of the Wilson Action	52
6.1	Eguchi–Kawai Model	52
6.2	Strong coupling expansion	57

7	Comparison with results from Montecarlo simulations	58
7.1	$n_t = 1$ in (3+1) dimensions	59
7.2	2+1 dimensions	60
7.3	$n_t > 1$ in (3+1) dimensions	61

1 Introduction

In the last twenty years the lattice regularization has proved to be a very powerful tool to understand and describe the non-perturbative features of non-abelian gauge theories. However, while impressive results have been obtained by means of Montecarlo simulations, very few progresses have been achieved with analytic techniques. Lattice Gauge Theories (LGT in the following) can be solved exactly in two dimensions for any gauge group, but become unaffordably complex in more than two dimensions, even in absence of quarks. Moreover, most of the approximation techniques which are usually successful in dealing with simpler statistical mechanical systems, like (suitably improved) mean field methods or strong coupling expansions turn out to be less useful in the case of LGT. A remarkable exception to this state of art is represented by the large N approximation [1] which is able to keep the whole complexity of the finite N models. Unfortunately, even in the large N limit (despite the fact that, as we shall discuss below, some major simplifications occur) it is not possible to give exact solutions (the so called “Master Field”) to the Lattice $SU(N)$ models. Notwithstanding this, several interesting results have been obtained in the past years even without the explicit knowledge of the Master Field.

In this review we shall deal with one of the most interesting features of non abelian gauge theories: the presence of a deconfinement transition at finite temperature. We shall apply large N techniques to finite temperature LGT, with the aim of constructing the phase diagram of the model, locate the critical points and identify their order. We shall deal for most part of the review with the pure gauge theory (namely without quarks); only in section 5.2 we shall comment on the phase diagram in presence of quarks. We shall keep d , the number of space-like dimensions as a free parameter, and shall study in particular the cases $d = 2$ and $d = 3$ which are the most interesting from a phenomenological point of view and for which there exist Montecarlo simulations to compare with our predictions.

This paper is an update rather than a complete review on this topic. We shall mainly concentrate on the most recent results (say, of the last five years). There are some very good reviews both on lattice gauge theories and on large N models which cover most of the results obtained up to the second part of the eighties. In particular, for the large N approach we suggest the reviews of S. Coleman [2], S.R. Das [3] and the recent contribution of Camprostrini, Rossi and Vicari [4]. For a throughout introduction to Lattice Gauge Theories, with a good discussion both of the large N limit and of the finite temperature regularization, we refer to [5].

During the eighties most of the efforts in the study of finite temperature large N LGT were devoted in the following two directions: *a)* Eguchi–Kawai (EK) type [6] models; *b)* dimensionally reduced model. Both these approaches have advantages and drawbacks. Twisted or Quenched EK models maintain the whole complexity of the theory and reduce it to models of just $(d+1)$ independent matrices. However these models could not be solved exactly, and the only fruitful approach has been so far to extract numerical results by using Montecarlo simulations. We shall discuss

below some of these results. Let us mention here that the reliability of Montecarlo simulations based on the TEK model is strongly affected by the presence of a first order bulk phase transition which shadows the true deconfinement transition. Finding a precise characterization of the TEK or QEK phase diagram, from the results of the Montecarlo simulations only, is a difficult and open problem.

On the other side, by doing some rather crude approximation, it has been possible to construct dimensionally reduced matrix models which are exactly solvable. The price to pay in this case is that the simplifications needed to reach the exact solvability are so strong that the resulting models show sometimes only a very faint similarity with the original models.

In the last few years it has been realized that some insight into the large N structure of LGT can be obtained by using the results that have been accumulating in the meantime on the large N solution of a variety of matrix models. These models have found important applications in various contexts. Let us mention among the others: the random matrix description [7] of various physical systems (ranging from quantum wires to chaotic systems), the exact solution of two dimensional LGT's [8, 9, 10, 11] and the related string like behaviour [12], the large N matrix approach to two dimensional quantum gravity [13] and the "induced QCD" models proposal by Kazakov and Migdal [14].

The present review is mostly concerned with the results [15, 16, 17, 18] obtained in the last few years in finite temperature LGT by using the matrix models techniques mentioned above. We shall show that by using both some recent results of two dimensional QCD and the exact solution [19] of the induced QCD models in any dimension, one can solve dimensionally reduced models (of the type b) listed above) that involve far less crude approximations than those discussed in the eighties. By using these exact results we can also solve, within a very good approximation, a simplified TEK model and understand its phase diagram. Our results can be compared with those obtained with Montecarlo simulations in the $N = 2$ and $N = 3$ cases. There are by now many rather precise numerical estimates of the deconfinement temperature for these models both in $d = 2$ and $d = 3$. We shall show that our results are rather good if compared with the simulations at $d = 2$, while they are in general poor (except for the lowest values of n_t , the lattice size in the time direction) in $d = 3$. We shall give some arguments to explain this failure and indicate how our results could be improved. Let us stress however that our aim is not to compete with the Montecarlo simulations, which certainly remain the most powerful tool to obtain quantitative result in LGT. Our idea is rather that any new analytic result in this context can teach us quite a lot on the non-perturbative regime of non abelian gauge theories. Moreover, even if our results are often only crude approximations of the exact ones, the pattern of the phase diagram that we obtain has good chances to be the correct one. Finally let us stress that there are situations in which the methods discussed here could even become competitive with the Montecarlo simulations. This is the case, for instance, when the model contains more that one coupling constant (like the mixed fundamental-adjoint action), and

the phase diagram is so complex that it is difficult to study it numerically.

The paper is organised as follows. For the sake of being as self-contained as possible, we devote a rather large introductory section (sec. 2) to describe the general setting of finite temperature LGT in a form which is suitable for our purposes. In sec. 3 we review in some detail the derivation of refined effective action for the Polyakov loops, both in the case of a LGT described by the heat kernel action and by the Wilson action. In sec. 4 the heat kernel effective model is discussed; its phase diagram is described, and a numerical estimate for the deconfinement temperature is obtained. In sec. 5 the phase diagram is re-discussed as a function of the space dimensionality and in the case in which the gauge fields are coupled to certain external static sources or to an external “magnetic” field. Sec. 6 is devoted to the analysis of the effective model obtained from the Wilson action; in particular we discuss its twisted reduction á la Eguchi–Kawai, that gives rise to a very interesting one-plaquette matrix model. In sec. 7 the results for the deconfinement temperature are discussed and compared with the available Montecarlo simulations.

2 General Setting

2.1 Asymmetric Lattices

Let us consider a finite temperature lattice gauge theory (LGT) with gauge group $SU(N)$, defined on a $d + 1$ dimensional cubic lattice. In order to describe a finite temperature theory we require that one dimension (which we shall call “time” from now on) is compactified with periodic boundary conditions and compactification length $\frac{1}{T}$, if T is the temperature. We shall assume that in the other “space” dimensions the extension of the lattice is infinite, or anyway much greater than $\frac{1}{T}$. If we denote by N_t the number of lattice spacings in the time direction, and a_t the corresponding lattice spacing, then we have $\frac{1}{T} = N_t a_t$. It is convenient to work with an asymmetric lattice, namely with different lattice spacing in the time and space directions. Let us denote by a_s the lattice spacing in the space directions. The ratio between a_t and a_s defines the asymmetry parameter ρ :

$$\rho = \frac{a_s}{a_t} = T N_t a_s . \quad (1)$$

We shall require that different values of ρ correspond to different, but equivalent, lattice regularization of the same model. In order to implement such requirement we introduce different bare couplings in the time and space directions. Let us call them β_t and β_s respectively. The Wilson action is then

$$S_W = N^2 \sum_{\vec{x}, t} \left(\sum_i \beta_t \hat{G}_{0i}(\vec{x}, t) + \sum_{i < j} \beta_s \hat{G}_{ij}(\vec{x}, t) \right), \quad (2)$$

where here and in what follows we denote by G_{0i} and G_{ij} the time-like and space-like plaquette variables:

$$\begin{aligned} G_{0i}(\vec{x}, t) &= V(\vec{x}, t)U_i(\vec{x}, t+1)V^\dagger(\vec{x} + \hat{i}, t)U_i^\dagger(\vec{x}, t) , \\ G_{ij}(\vec{x}, t) &= U_i(\vec{x}, t)U_j(\vec{x} + \hat{i}, t)U_i^\dagger(\vec{x} + \hat{j}, t)U_j^\dagger(\vec{x}, t) \end{aligned} \quad (3)$$

and by $\hat{G}_{0i}(\vec{x}, t)$ and $\hat{G}_{ij}(\vec{x}, t)$ the real part of the suitably normalized traces:

$$\hat{G}_{0i}(\vec{x}, t) = \frac{1}{N} \text{Re Tr } G_{0i}(\vec{x}, t) , \quad \hat{G}_{ij}(\vec{x}, t) = \frac{1}{N} \text{Re Tr } G_{ij}(\vec{x}, t) . \quad (4)$$

In eq. (3) we have denoted by $U_i(\vec{x}, t)$ the link variables in the space directions ($i \in \{1, 2, \dots, d\}$) and by $V(\vec{x}, t)$ the link variables in the time direction. The components of \vec{x} and t are integers, with t periodic modulo N_t . The normalization of the couplings β_s and β_t has been chosen, by extracting a N^2 factor in front of S_W , in such a way to have a smooth large N limit.

For a given ρ the relation between the bare couplings β_t and β_s can be obtained by requiring that the Wilson action (2) reproduces in the naive continuum limit a gauge theory with the same coupling constant g for all components of the field strength. This leads to the following equations, which relate ρ and the bare gauge coupling g to β_t and β_s :

$$\frac{2}{Ng^2} = a_s^{3-d} \sqrt{\beta_s \beta_t} , \quad \rho = \sqrt{\frac{\beta_t}{\beta_s}} . \quad (5)$$

It is clear from eqs. (1) and (5) that equivalent regularizations with different values of ρ require different values of N_t . Hence, to maintain the equivalence, N_t must be a function of ρ according to eq. (1).

Among all these equivalent regularizations a particular role is played by the symmetric one, which is defined by:

$$\beta \equiv \frac{2}{Ng^2} a^{d-3} \quad (6)$$

(from now on we shall distinguish the symmetric regularization from the asymmetric ones by eliminating the subscripts t and s in β and a). By comparing eq.s (1,5,6) we see that all regularizations are equivalent to a symmetric one provided

$$\beta = \rho \beta_s = \frac{\beta_t}{\rho} , \quad (7)$$

$$N_t(\rho) = \rho n_t , \quad (8)$$

where n_t is the number of links in the time direction with a symmetric regularization: $n_t = N_t(\rho = 1)$.

Notice however that these equivalence relations have been derived in the *naive* or “classical” continuum limit, and quantum corrections are in general present. These

corrections were studied and calculated in the (3+1) dimensional case by F.Karsch in [20]. They lead to the following expressions:

$$\beta_t = \rho(\beta + c_\tau(\rho)) , \quad (9)$$

$$\beta_s = \frac{\beta + c_\sigma(\rho)}{\rho} . \quad (10)$$

The quantum effects are encoded in the two functions $c_\sigma(\rho)$ and $c_\tau(\rho)$ ¹. We shall be interested in their behaviour at large ρ , that can be extracted from [20] and is given by the asymptotic expansion:

$$c_{\sigma,\tau} \equiv \alpha_{\sigma,\tau}^0 + \frac{\alpha_{\sigma,\tau}^1}{\rho} + \dots . \quad (11)$$

The numerical values of the α 's in the large N limit can be obtained from [20], and they are given by: $\alpha_\tau^0 = -0.2629$; $\alpha_\tau^1 = 1/4$; $\alpha_\sigma^0 = 1/4$; $\alpha_\sigma^1 = 1/4$.

2.2 Center symmetry and the Polyakov loop

The major consequence of the periodic boundary conditions in the time direction is the appearance of a new global symmetry of the action, with symmetry group the center C of the gauge group (in our case \mathbf{Z}_N).

This symmetry can be realized as follows. Let us transform all the timelike links of a given space-like slice with the same element W_0 belonging to the center of the gauge group.

$$V(\vec{x}, t) \rightarrow W_0 V(\vec{x}, t) \quad \forall \vec{x}, \quad t \text{ fixed} . \quad (12)$$

The space-like plaquettes are not affected by the transformation, while in each timelike plaquette two contribution appear: W_0 and W_0^{-1} . Since they belong to the center, they commute with all other matrices in the plaquette and can be moved so as to cancel each other. So the Wilson action is invariant under such transformation. The important point is that, due to the periodic boundary conditions in the time direction, it is impossible to re-absorb this global twist by means of local gauge transformations..

A second consequence of the periodic boundary conditions is that it is possible to define gauge invariant observables which are topologically non-trivial. The simplest choice is the Polyakov loop, defined in terms of link variables as:

$$\hat{P}(\vec{x}) \equiv \text{Tr} \prod_{t=1}^{N_t} V(\vec{x}, t) . \quad (13)$$

¹Let us notice, to avoid confusion, that our functions c_σ and c_τ correspond to those of [20] multiplied by the factor $2/N$, which ensures a smooth limit as $N \rightarrow \infty$.

In the following we shall often use the untraced quantity $P(\vec{x})$, defined as:

$$P(\vec{x}) \equiv \prod_{t=1}^{N_t} V(\vec{x}, t) , \quad (14)$$

which will be referred to as ‘‘Polyakov line’’.

The relevant feature of the Polyakov loop is that it transforms under the above discussed symmetry as follows:

$$\hat{P}(\vec{x}) \rightarrow W_0 \hat{P}(\vec{x}) ; \quad (15)$$

thus it is a natural order parameter for this symmetry. It will acquire a non zero expectation value if the center symmetry is spontaneously broken. In a pure LGT the Polyakov loop has a deep physical interpretation, since its expectation value is related to the free energy of a single isolated quark.

Hence the fact that the Polyakov loop acquires a non-zero expectation value can be considered as a signature of deconfinement and the phase transition which separates the regime in which the center symmetry is unbroken from the broken symmetric phase will be the deconfinement transition.

General arguments show that, in $d > 1$, finite temperature gauge theories admit such a deconfinement transition for some critical value of the temperature $T = T_c$, separating the high temperature, deconfined, phase ($T > T_c$) from the low temperature, confining domain ($T < T_c$). In the following we shall be interested in the phase diagram of the model as a function of T , and we shall make some attempt to locate the critical point T_c .

A peculiar feature of the behaviour of the Polyakov loop in the high temperature phase is that its (non-zero) expectation value is *not* a generic element of $SU(N)$ but tends to fluctuate around one of the elements of the center. These fluctuations become smaller and smaller as the temperature increases and finally in the infinite temperature limit the expectation value of the Polyakov loop *exactly* becomes an element of C (see for instance [21] for a discussion of this point).

This feature will be relevant in the following, when we shall describe these small fluctuations of the Polyakov loop in the high temperature phase by using a suitable generalization of the Kazakov–Migdal model.

2.3 Svetitsky–Yaffe conjecture

The peculiar role played by the Polyakov loops in the above discussion, suggests to use some kind of effective action for the Polyakov loops to study the deconfinement transition and, more generally, the physics of finite temperature LGT.

Let us make this statement more precise. Constructing an *exact* effective action for the Polyakov loops, equivalent to the original LGT is clearly impossible (even in the simplest possible, non-trivial, LGT, namely the (2+1) dimensional Ising gauge model) since it would require to integrate out exactly all the space-like gauge degrees

of freedom of the original model. However one can try to approximate somehow this integration and, at the same time, treat exactly the timelike degrees of freedom which are related to the Polyakov loops. The discussion of sec. 2.2 then tells us that this type of approximation is the one which better preserves the finite temperature behaviour of the original model. The resulting *approximate* effective action will keep *all* the symmetries of the original model relevant to the deconfinement dynamics and as a consequence it will give a faithful *qualitative* description of this transition. We can also hope to have a *quantitative* agreement between the results obtained with the effective action and those of the gauge model. This agreement will become better and better as we improve our approximation in the space-like degrees of freedom.

This approach was proposed and discussed in [21] and accordingly we shall refer to it, in the following, as the “Svetitsky–Yaffe program”. The most appealing feature of this program is that, by resorting only to some general results of statistical mechanics, before doing any calculation, one can obtain several interesting predictions on the phase diagram of the model. Let us see some of them:

- a) If the original gauge theory lives in $(d+1)$ dimension, then the effective theory for the Polyakov loops is a d -dimensional spin system with symmetry group the center C of the original gauge group.
- b) The deconfinement transition of the original gauge model becomes the order–disorder transition of the effective spin system. The ordered phase of the spin model corresponds to the deconfined phase in the original gauge theory. In this phase the Polyakov loop acquires a non-zero expectation value.
- c) This effective theory would obviously have very complicate interactions, but Svetitsky and Yaffe were able to argue that all these interactions should be short ranged. As a consequence, if the deconfinement transition of the original gauge model (and hence of the effective spin model) is continuous, near this critical point, where the correlation length becomes infinite, the precise form of the short ranged interactions should not be important.
- d) Let us consider now the much simpler spin model with only nearest neighbour interactions and the same global symmetry group. If also the order-disorder phase transition of this model is continuous then, due to point (c) above, its universality class should coincide with that of the deconfinement transition.

This last result is usually known as the “Svetitsky–Yaffe conjecture”, and has been confirmed in the last years by several Montecarlo simulations. It is certainly the most important consequence of this whole approach.

Let us stress again that it applies only to the case in which *both* the deconfinement transition of the gauge model and the order-disorder transition of the nearest neighbour effective spin model are continuous. So it does not apply in our case

since in the effective actions that we shall study in the following the order-disorder transition turns out to be of the first order.

There are however, in our large N limit framework two other intriguing questions which are raised by the SY analysis. The first one refers to the difference between the deconfinement transition in \mathbf{Z}_N and $SU(N)$ LGT's. Both have the same center \mathbf{Z}_N so they should be described by the same effective spin model. However we know very well that the two LGT's have rather different features. This differences becomes particularly evident in the large N limit where in one case we have the $U(1)$ LGT which, for instance, in (2+1) dimensions is always confining, while in the other case one finds the large N deconfinement transition which will be the subject of the forthcoming sections.

A second, related, problem is that, according to the SY point of view, the deconfined phase should correspond to the ordered phase of the effective spin model, but in two dimensions the Mermin–Wegner theorem [23] tells us that the fluctuation are always strong enough to restore the $U(1)$ symmetry thus forbidding the existence of an ordered phase and consequently of a deconfined phase in the original (2+1) LGT. This prediction is in clear contradiction with the analysis of the present paper and also with the commonly accepted scenario for non-abelian LGT's in (2+1) dimensions.

2.4 \mathbf{Z}_N versus $SU(N)$

In this subsection we shall try to answer these questions and to better understand the difference between \mathbf{Z}_N and $SU(N)$ LGT's. Let us start our discussion with the analysis of the \mathbf{Z}_N models, which are simpler. In this case one easily realizes that the nearest neighbour effective spin model which describes the Polyakov loops dynamics is the \mathbf{Z}_N symmetric “clock model”. Its phase diagram in $d = 2$ is well known [22]. It is rather non trivial and admits, for finite N and large enough β , an ordered phase in which the \mathbf{Z}_N symmetry is spontaneously broken. In fact the phase diagram of the \mathbf{Z}_N models (if $N > 4$) is composed by three phases: the usual (low β) disordered and (high β) ordered phases and a new intermediate phase which is critical and has the same features of the high β phase of the $U(1)$ model. This intermediate phase is separated from the high and low β phases by two phase transitions of the Kosterlitz–Thouless [24] (KT) type. The \mathbf{Z}_N model in two dimensions is self dual, and this greatly simplifies the study of the phase diagram. Ordered and disordered phases are related by duality (just like in the well known 2d Ising model) and also the two KT transitions are dual to each other [22]. The coupling of the dual theory is related to the inverse of the original one by a factor N^2 . As N increases, the location of the first KT transition (the one which divides the disordered from the critical phases) remains more or less unchanged, and as $N \rightarrow \infty$ it becomes the KT transition of the $U(1)$ model, whose critical coupling β_{KT} is of order unity. The other KT transition and the ordered phase, which begins at this KT transition, due to the N^2 factor mentioned above, are pushed to infinity

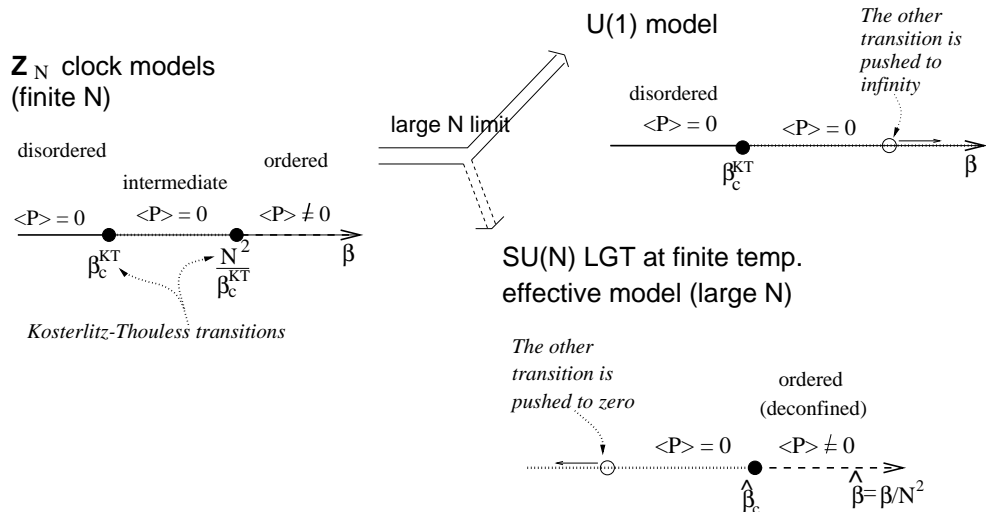


Fig. 1: Relation between the phase diagrams of the \mathbf{Z}_N “Clock models”, the $U(1)$ model and the effective model for the Polyakov loops in large N LGT at finite temperature. When taking the large N limit of the \mathbf{Z}_N models, depending if the coupling constant is rescaled with $1/N^2$ (LGT case) or not ($U(1)$ case), one of the two Kosterlitz–Thouless transitions of the \mathbf{Z}_N models is pushed to infinity or to zero, respectively, and disappears for $N = \infty$.

as N increases, and finally, in the $N \rightarrow \infty$ limit, disappear. This agrees with the $U(1)$ phase diagram discussed above, which in fact does not admit an ordered phase. This discussion suggests that in the large N limit the $(2+1)$ dimensional \mathbf{Z}_N LGT can never have a truly deconfined phase, and that the fluctuations of the Polyakov loops are always strong enough to restore the $U(1)$ symmetry.

In the $SU(N)$ case the global symmetry of the effective spin model is again \mathbf{Z}_N , but the model is much less trivial. In each site instead of a single spin which can take N values we have a collection of N spins (the eigenvalues of the $SU(N)$ matrix) and the nearest neighbour effective action between these collections of spins is highly non trivial. If we label the eigenvalues with an index i then the action, which, according to the SY conjecture, is local in the real space, turns out to be non local in the index space. It is exactly this last feature which makes the difference and allows the existence of a high β phase in which the Polyakov loop expectation value is different from zero. Once the large N limit has been taken and a master field configuration for the eigenvalues has been assumed, it turns out to be very difficult to understand how the non locality in the index space could allow to circumvent the Mermin–Wegner theorem. However, the above discussion on the phase diagram of the \mathbf{Z}_N models allows us to gain some intuition of this phenomenon from a different point of view and, in particular, to see that there is no contradiction between the SY conjecture and the presence of a deconfined phase in the large N limit of $SU(N)$ LGT’s.

In fact, let us take a value of N large, but finite and let us assume that for large β the $SU(N)$ LGT admits a deconfined phase. This means that all the Polyakov loops are “frozen” in the same direction (one of the \mathbf{Z}_N roots of unity). If β is large enough all the eigenvalues (namely all the spins in each given site) take the same value and the non-locality in the index space becomes trivial. The effective action becomes N^2 times the action of the \mathbf{Z}_N clock model². This means that the critical coupling which separates the deconfined (i.e. ordered, in the language of the \mathbf{Z}_N model) phase from the intermediate phase scales³ with N^2 . Thus we are exactly in the region where the \mathbf{Z}_N clock model admits a broken symmetric phase and we see explicitly that there is no contradiction between our assumption of the presence of a deconfined phase and the SY dimensional reduction. Moreover we see that we can take smoothly in both models (LGT and spin model) the large N limit and keep the agreement between the two phase diagrams.

This allows us to better understand the relation between $SU(N)$ and \mathbf{Z}_N LGT’s in (2+1) dimensions. For suitable values of β both have the same two-dimensional \mathbf{Z}_N spin model as effective action, but they are described by two very different regimes in the coupling space of the spin model.. Low β (of order unity) for the \mathbf{Z}_N LGT, high β (of order N^2) for the $SU(N)$ theories. This consideration shares some more light on the SY conjecture and explains how is it possible that gauge models, which have a very different dynamics (like the \mathbf{Z}_N and $SU(N)$ ones) could be described by the same effective action.

2.5 Character expansion in the large N limit

An important role in the following analysis will be played by the character expansion. Let us briefly summarize few results (for more details see Ref. [5]). We shall particularize them to the $SU(N)$ case, but most of them hold for any Lie group G and with minor modifications also for discrete groups. The irreducible characters $\chi_r(U)$ are the traces of the irreducible representations (labelled by r) of the group. They form a complete orthonormal basis for the class functions on the group. A function $f(U)$ on the group is called a “class function” if it satisfies the relation:

$$f(U) = f(VUV^\dagger) \quad \forall V \in SU(N) . \quad (16)$$

In particular, the characters themselves are class functions. The pure gauge action, eq. (2), is a class function.

²Let us stress that this is a simplified picture and that fluctuations in the eigenvalues distribution are present for any finite value of β . These fluctuations are very important in the discussion of the phase diagram of the theory and we shall deal with them in sec. 4. But with respect to the present discussion they only represent a higher order correction and do not affect the validity of the argument.

³ This is already apparent in the definition of the coupling (see eq. (2)) where we have factorized a N^2 factor to ensure a smooth $N \rightarrow \infty$ limit.

The following orthogonality relations between characters hold:

$$\int DU \chi_r(U) \chi_s^*(U) = \delta_{r,s} , \quad (17)$$

$$\sum_r d_r \chi_r(U V^\dagger) = \delta(U, V) , \quad (18)$$

where DU denotes the Haar measure (normalized to unity) on $SU(N)$ and d_r denotes the dimension of the r^{th} representation.

Besides the above orthogonality relations we shall make use of two important integration formulas of the characters, namely:

$$\int DU \chi_r(V_1 U) \chi_s(U^\dagger V_2) = \delta_{r,s} \frac{\chi_r(V_1 V_2)}{d_r} ; \quad (19)$$

$$\int DU \chi_r(U V_1 U^\dagger V_2) = \frac{1}{d_r} \chi_r(V_1) \chi_r(V_2) . \quad (20)$$

Any class function can be expanded in the basis of the characters:

$$f(U) = \sum_r \chi_r(U) f_r , \quad (21)$$

where the sum is over the set of all irreducible representations of the group, and the coefficients f_r are given by

$$f_r \equiv \int DU \chi_r^*(U) f(U) . \quad (22)$$

Let us construct now the character expansion for the Wilson action.

The Boltzmann factor associated to each plaquette in the Wilson action is (we neglect the index “ t ” or “ s ” of β , which is irrelevant for the following analysis) :

$$e^{N\beta \text{ReTr}G} = \sum_r F_r(\beta) \chi_r(G) , \quad (23)$$

where G , given by eq. (3) above, denotes the ordered product of the link variables around the plaquette and the coefficients F_r are given by:

$$F_r(\beta) \equiv \int DU e^{N\beta \text{ReTr}U} \chi_r^*(U) = \sum_{n=-\infty}^{\infty} \det I_{r_j - j + i + n}(N\beta) . \quad (24)$$

The r_j 's are a set of integers labelling the representation r and they are constrained by: $r_1 \geq \dots \geq r_N = 0$. The indices $1 \leq i, j \leq N$ label the entries of the $N \times N$ matrix of which the determinant is taken and $I_n(\beta)$ denotes the modified Bessel function of order n .

As a consequence of the factor d_r at the denominator in eq.s (19, 20) the relevant coefficients in the character expansion (23), namely the ones that will appear in the

strong coupling expansions, are not the F_r themselves, but the following normalized coefficients:

$$D_r(\beta) = \frac{F_r(\beta)}{d_r F_0(\beta)} . \quad (25)$$

These coefficients have two remarkable properties, which will be important in the following:

- a)* In the large N limit they have a very simple form, if the limit is taken keeping $\beta < 1$ fixed:

$$\begin{aligned} F_0(\beta) &\sim e^{(\frac{N\beta}{2})^2} , \\ F_f(\beta) &\sim \frac{N\beta}{2} e^{(\frac{N\beta}{2})^2} , \end{aligned}$$

where the index f denotes the fundamental representation (whose dimension is N). The above relations imply that in the large N limit

$$D_f(\beta) = \frac{\beta}{2} . \quad (26)$$

Similar simplified relations hold also for higher representations.

- b)* For any fixed value of N , in the large β limit the coefficients D_r become equivalent to the heat kernel coefficients:

$$\lim_{\beta \rightarrow \infty} D_r(\beta) = e^{-\frac{C_r}{2N\beta}} , \quad (27)$$

where C_r denotes the quadratic Casimir in the r^{th} representation. As it is easy to see, this exponential form greatly simplifies the construction of strong coupling expansions. Moreover, this limit is particularly relevant for us, since this is exactly the situation that we have for the timelike part of the action when the asymmetry parameter ρ is sent to infinity.

2.6 Scaling behaviour

The ultimate test of the correctness of any lattice regularization is that, as the continuum limit is approached, the various dimensional quantities follow the correct scaling behaviour. This scaling behaviour can be easily obtained by writing explicitly the dependence on the lattice spacing a of the relevant (dimensional) observables. The form of these scaling laws depends on the number of spacetime dimensions of the lattice. So we shall discuss separately the two cases $d = 2$ and $d = 3$ which are the most relevant ones for the physical applications. We shall concentrate in particular on the scaling behaviour of the critical temperature T_c (which has the dimension of a mass) since this is the simplest physical observable

which we can study with our techniques. We shall be interested in the scaling laws as functions of the coupling β and of the lattice size in the time direction N_t . We shall study for simplicity the case of a symmetric lattice $\beta_s = \beta_t \equiv \beta \equiv \frac{4}{g^2}$. If $\rho \neq 1$, the change in the scaling laws due to the asymmetry is completely encoded in the equations (9) and (10) and in the functions $c_\sigma(\rho)$ and $c_\tau(\rho)$ discussed in sec. 2.1.

2.6.1 $d=2$

In the $d = 2$ case the coupling constant g^2 has the dimensions of a mass (see eq. (6)). This simplifies the analysis since in this case the coupling constant itself sets the overall mass scale. So near the continuum limit a physical observable, like T_c , with the dimensions of a mass can be written, according to the renormalization group equations, as a series in powers of g^2 . Hence in terms of the coupling β we have:

$$aT_c = \frac{a_1}{\beta} + \frac{a_2}{\beta^2} + \dots . \quad (28)$$

The critical temperature is obtained by looking at the critical coupling β_c at which the deconfinement transition occurs; hence, if the lattice size in the time direction is $N_t \equiv \frac{1}{Ta_t}$, we can rephrase eq. (28) as a scaling law for the behaviour of the critical coupling β_c as a function of N_t . Keeping only the first term in eq. (28) we find:

$$\beta_c(N_t) = a_1 N_t . \quad (29)$$

Thus from the simple observation that in (2+1) dimensions g^2 has dimensions of a mass we immediately deduce that near the continuum limit β_c must be a *linear* function of N_t . If the lattice is asymmetric we can use eq.s (9) and (10) to reconstruct the equivalent symmetric coupling and then use again eq. (29).

2.6.2 $d=3$

This case is less trivial, since by looking at eq.s (5, 6) we see that for $d = 3$ the coupling constant g^2 is dimensionless and the theory dynamically generates a dimensional scale Λ_L in units of which we must measure any dimensional quantity on the lattice. The dependence of the lattice spacing on β can be reconstructed in the continuum limit by using the renormalization group equations. The well known two loop result is:

$$a\Lambda_L = (b_0 g^2)^{-\frac{b_1}{2b_0^2}} \exp\left(-\frac{1}{2b_0 g^2}\right) , \quad (30)$$

where b_0, b_1 are the first two coefficients of the Callan–Symanzik equation which for $SU(N)$ are:

$$b_0 = \frac{11N}{48\pi^2} , \quad b_1 = \frac{34}{3} \left(\frac{N}{16\pi^2}\right)^2 . \quad (31)$$

Plugging eq. (30) into the definition of the critical temperature:

$$T_c = \frac{1}{aN_t}, \quad (32)$$

we find:

$$\frac{T_c}{\Lambda_L} = \frac{1}{N_t} \left(\frac{24\pi^2\beta}{11} \right)^{-\frac{51}{121}} \exp \left(\frac{12\pi^2\beta}{11} \right). \quad (33)$$

If the continuum limit is correctly taken then the ratio T_c/Λ_L should approach for large enough values of β (hence, in our case, also for large values of N_t) a constant value. Inserting this constant into eq. (33) and keeping only the first perturbative contribution in eq. (30) we immediately see that, for $d=3$, β_c is a *logarithmic* function of N_t .

3 Construction of the Effective Action

The aim of this section is to construct an effective action for the finite temperature LGT in terms of Polyakov loops only. In agreement with the Svetitsky–Yaffe program outlined above, we shall try to integrate over the space-like variables $U_i(\vec{x}, t)$ in the Wilson action (2) so that the only remaining degrees of freedom will be at the end the Polyakov loops. The resulting effective action will live in d dimensions, one dimension less than the starting model. The integration over the space-like variables can be done in principle in two distinct steps. First one integrates over all the space link variables except for the ones on an arbitrarily chosen time layer. The result is a lattice theory with $N_t = 1$ in which the time-like links are the open Polyakov loops. This first step will be denoted for obvious reasons as “dimensional reduction”. The second and last step consists in the integration over the remaining space-like link variable, leading to an effective action with the Polyakov loops as the only dynamical variables. As already remarked in the introduction the integration over the space-like variables cannot be performed exactly and some approximation is needed. The approach that we shall follow consists in treating the time-like part S_t of the Wilson action as a Born term and the space-like part S_s as a perturbation. This means making a strong coupling expansion in β_s while treating the time-like part of the action exactly. The first term of this expansion, which we shall call in the following “zeroth order approximation” simply corresponds to neglecting the space-like plaquettes. In this case both steps in the integration over the space-like links can be performed exactly, at least as a character expansion, but the result is in some respect unsatisfactory. In this limit in fact the result is exactly the same that one would obtain with a standard Migdal–Kadanoff [25] bond-moving approximation and it has the same drawbacks. In fact, in $3+1$ dimensions, it gives a good approximation of the whole theory only for $N_t = 1$ while for larger N_t ’s, although it still gives a good *qualitative* description of the phase diagram, it fails to predict the critical properties of the deconfinement transition, namely the scaling

behaviour of the critical coupling β_c as a function of N_t . This is a major problem, since it is only by following the correct scaling behaviour that one can finally take the continuum limit and extract, for instance, a reliable estimate for the deconfinement temperature. The situation is different in $2 + 1$ dimensions where, at least to the leading order N_t , the scaling behaviour of the “zeroth order approximation” and of the full theory coincide. As a consequence we may expect that the “zeroth order approximation” gives in this case reliable results even at large values of N_t . Qualitatively the picture is the following: in $3 + 1$ dimensions the statistical weight of the space-like plaquettes is large enough to affect the scaling properties; hence they can be neglected only for small values of N_t , where the critical value of β is small and the correlations between Polyakov loops induced by the space-like plaquettes negligible. On the contrary in $2 + 1$ dimensions the weight of the space-like plaquettes is too small to affect the scaling, and there are a good indications that they are not important not only for small N_t but also near the continuum limit.

The effect of the space-like plaquettes can be taken into account perturbatively, order by order in β_s . In [26] we constructed the first non trivial order in β_s for the SU(2) model and indeed found a better agreement with the expected scaling law in $d = 3$. Unfortunately the effective action at this order becomes very cumbersome, no exact solution can be found and one has to rely on mean field estimates of the critical coupling. Moreover, it is easy to see that the complexity of the calculations further increases as higher orders are taken into account or if larger values of N are considered.

In the large N limit a completely different approach, which is more elegant and powerful, is available. By using suitable modifications of the Eguchi–Kawai techniques it is possible to perform an exact dimensional reduction, and obtain an action with $N_t = 1$ *which is completely equivalent to the original Wilson action*. Although the last step, namely the integration over the remaining space-like link variables, still proves to be too difficult, this is a major improvement with respect to previous approaches. In particular, as discussed in detail in sec. 6, the solution of the dimensionally reduced action in the $\beta_s = 0$ limit gives the next to leading order in the scaling behaviour of β_c , which turns out to be in excellent agreement, in $2 + 1$ dimensions, with the available Montecarlo simulations.

This section is divided into two parts. In the first one (sec. 3.1) we review the construction of the “naive” effective actions, namely the ones obtained with the “zeroth order approximation”. In sec.s 3.1.1 and 3.1.2 we shall construct respectively the zeroth order approximation of the heat kernel action (which can be thought of as the $\rho \rightarrow \infty$ limit of the standard Wilson action) and of the Wilson action itself. Then we shall obtain the corresponding scaling behaviours (sec. 3.1.3), and we shall discuss the reasons why they are unsatisfactory. Finally we shall describe a simplified version of the effective action (sec. 3.1.4), which is simple enough to be solved exactly and at the same time accurate enough to give a good *qualitative* description of the phase diagrams of the deconfinement transition. All the material collected in this first part is rather old. It mainly refers to results already obtained at the

beginning of the eighties, even if they are discussed here in the new framework of our strong coupling expansion.

On the contrary, in the second part we deal with some completely new results. First we shall discuss how to construct higher order terms in the β_s expansion (sec. 3.2.1). We shall also show that, in spite of the N^2 factor in front of the space-like coupling, the expansion in powers of β_s is convergent order by order in the large N limit. This is a non-trivial and important check of the consistency of the strong coupling expansion in β_s . Finally in sec. 3.2.2 we shall derive an exact dimensional reduction by using techniques typical of the Eguchi–Kawai models.

3.1 Naive dimensional reduction ($\beta_s = 0$) and related effective actions.

The starting point for our considerations is the complete action S_W defined in (2) on a lattice with arbitrary asymmetry parameter ρ . More precisely we shall consider

$$e^{S_W} = \prod_{\vec{x}, t, i} \left\{ \sum_r d_r D_r(\beta_t) \chi_r(G_{0i}(\vec{x}, t)) \right\} e^{N^2 \sum_{i < j} \beta_s \hat{G}_{ij}(\vec{x}, t)}, \quad (34)$$

where a character expansion of the contributions of the time-like plaquettes has been performed according to eq.s (23) and (25). The naive dimensional reduction can be achieved by simply setting $\beta_s = 0$ in (34). In this case it is easy to integrate out the space link variables $U_i(\vec{x}, t)$. This can be done exactly because each link variable $U_i(\vec{x}, t)$ belongs only to two timelike plaquettes. In fact, consider the ladder of plaquettes obtained from any given timelike plaquette by moving in the time direction. Its contribution to the action is:

$$A(\vec{x}, i) \equiv \prod_t \left\{ \sum_r d_r D_r(\beta_t) \chi_r(G_{0i}(\vec{x}, t)) \right\}. \quad (35)$$

The integration over the first $N_t - 1$ space-like link variables on the ladder can be done by using eq. (19), leading to the following result:

$$\sum_r d_r [D_r(\beta_t)]^{N_t} \chi_r \left(U_i(\vec{x}, t = 0) P(\vec{x} + \hat{i}) U_i^\dagger(\vec{x}, t = N_t) P^\dagger(\vec{x}) \right). \quad (36)$$

The effect of this integration is to reduce the original action (which had N_t space-like slices in the time direction) to an effective action with only one link in the timelike direction and one space-like slice. The timelike plaquettes of this reduced action are very peculiar: the two space-like links coincide due to the periodic boundary conditions, while the two timelike links exactly correspond to the Polyakov lines defined in eq. (14), which are indeed the degrees of freedom which we are interested in to construct our effective action.

The last step is now to integrate the remaining space-like links. Because of the periodicity in the time direction this integration is of the type given in (20).

By repeating the same procedure to all ladders the integration over all space-like link variables can be explicitly performed, leading to the following effective action for the Polyakov loops at $\beta_s = 0$:

$$\begin{aligned} e^{S_{\text{Pol}}(\beta_s=0)} &= \int \prod_{\vec{x}, t, i} DU_i(\vec{x}, t) \left\{ \sum_r d_r \chi_r [D_r(\beta_t)]^{N_t} (G_{0i}(\vec{x}, t)) \right\} \\ &= \prod_{\vec{x}, i} \sum_r [D_r(\beta_t)]^{N_t} \chi_r(P(\vec{x} + \hat{i})) \chi_r(P^\dagger(\vec{x})) . \end{aligned} \quad (37)$$

Notice that up to eq. (36) we were still dealing with an ordinary (even if asymmetric) lattice gauge theory. With the last integration, the gauge theory disappears and we end up with a spin model in one dimension less than the original model. However it is still possible to recognize some remnant of the original gauge symmetry in the invariance of the characters under transformations of the type $V \rightarrow W^{-1}VW$. Everything that has been done so far, in particular eq. (37), is valid for any value of the asymmetry parameter ρ . In the next subsections we shall consider the two extreme situations, namely $\rho = \infty$ and $\rho = 1$. It should be stressed that the effective actions obtained from (37) by setting $\rho = \infty$ and $\rho = 1$ are equivalent regularizations of the effective $\beta_s = 0$ theory in the continuum, but they differ away from the continuum limit.

3.1.1 $\rho \rightarrow \infty$ limit: heat kernel action

The large ρ limit of eq. (37) can be easily obtained from the asymptotic behaviour of the D_r coefficients given in (27), namely⁴

$$[D_r(\beta_t)]^{N_t} \xrightarrow{\rho \rightarrow \infty} \exp\left(-\frac{C_r n_t \rho}{2N \beta_t(n_t \rho)}\right) = \exp\left(-\frac{C_r n_t}{2N \beta_{\text{hk}}}(n_t)\right) , \quad (38)$$

where we have used the fact that $N_t = \rho n_t$, and defined a new coupling β_{hk} as

$$\beta_{\text{hk}}(n_t) = \lim_{\rho \rightarrow \infty} \frac{\beta_t(n_t \rho)}{\rho} \quad (39)$$

This new ‘‘heat kernel’’ coupling is related in the continuum limit, that is for large n_t , to the coupling β of the symmetric lattice by the relation (9)⁵:

$$\beta_{\text{hk}}(n_t) \stackrel{n_t \rightarrow \infty}{\sim} \beta(n_t) + \alpha_\tau^0 \quad (40)$$

⁴ β_t is a free parameter of the theory and as such is not related to N_t . It becomes a function of N_t if we require that as N_t changes the effective model (37) describes the same physics. This implies for instance that the expectation value of the Polyakov loop and of other observables does not depend on the value of N_t .

⁵Notice however that, since the space-like plaquettes have been neglected, the quantum corrections and hence the numerical values of $\alpha_\tau^{0,1}$ may be different from the ones given in sec. 2.1.

Away from the continuum limit, the effective action with $\rho = \infty$ and the one defined on a symmetric lattice are not analytically related, and β_{hk} should be regarded as an independent coupling. By inserting (38) into (37) we find

$$e^{S_{\text{Pol}}^{\text{hk}}(\beta_s=0)} = \prod_{\vec{x}, i} \sum_r \chi_r(P(\vec{x} + \hat{i})) \chi_r(P^\dagger(\vec{x})) \exp\left(-\frac{C_r n_t}{2N\beta_{\text{hk}}}\right), \quad (41)$$

which is the final form of the heat kernel ($\rho \rightarrow \infty$) effective action for the Polyakov loop.

3.1.2 Symmetric lattice: Wilson action

Let us consider now the case of a symmetric lattice ($\rho = 1$), which is particularly important if one wants to compare the analytic results with the results of Montecarlo simulations. The action is obtained from (37) by replacing β_t with the symmetric coupling β and N_t with n_t :

$$e^{S_{\text{Pol}}^{\text{W}}(\beta_s=0)} = \prod_{\vec{x}, i} \sum_r [D_r(\beta)]^{n_t} \chi_r(P(\vec{x} + \hat{i})) \chi_r(P^\dagger(\vec{x})), \quad (42)$$

As a consequence of eq. (38) the heat kernel and the Wilson effective actions, given by eq.s (41) and (42), coincide in the large β_{hk} and β limit provided the ratio of the two couplings goes to 1 in the continuum limit ($n_t \rightarrow \infty$). This is guaranteed by eq. (40) as the constant term α_τ^0 is negligible in that limit. Hence, as expected, the heat kernel and the Wilson effective actions have the same continuum limit. For finite n_t the two model are different and the coupling constants β_{hk} and β are in principle unrelated. However, in the strong coupling limit (small β), $S_{\text{Pol}}^{\text{W}}$ and $S_{\text{Pol}}^{\text{hk}}$ coincide again provided a suitable relation between the couplings of the two actions is established. In fact in that limit one retains in the character expansion of eq.s (41) and (42) only the contributions of the fundamental representation and its conjugate, which are the leading contributions in the strong coupling limit. A direct comparison of the formulas, taking into account eq. (26) and the relation $C_f^{(2)} = N$, gives:

$$\beta = 2 e^{-\frac{1}{2\beta_{\text{hk}}}} + \dots \quad (\beta, \beta_{\text{hk}} \rightarrow 0), \quad (43)$$

where the dots denote higher order corrections which vanish in the $\beta \rightarrow 0$ limit.

3.1.3 Scaling behaviours

This analysis and the knowledge of the explicit form of the two actions, allows us to obtain some general information on the scaling behaviour that we may expect for T_c . In the heat kernel case the result is very simple. It can be read directly from eq. (41) by requiring that the physics does not change if we simultaneously change β_{hk} and n_t . This implies a linear scaling of β_{hk} with n_t .

$$\beta_{\text{hk}}(n_t) = J n_t. \quad (44)$$

The “renormalized coupling” $J \equiv \beta_{\text{hk}}(n_t = 1)$ is the relevant parameter in the continuum limit; it will play a major role in the following.

In the Wilson case, due to the complicated form of the coefficients $D_r(\beta)$ the situation is less simple. However we can all the same deduce *asymptotic* scaling relations from the *exact* scaling of the heat kernel action (eq. (44)) and the relations between β and β_{hk} (eq.s (40,43)). Let us define also in the Wilson case a “renormalized coupling” J_W by setting $J_W = \beta(n_t = 1)$. We must distinguish then the weak coupling from the strong coupling regime. In the weak coupling the two actions coincide and also for the Wilson action we find a linear scaling. In fact by simply replacing eq. (44) into (40) we find:

$$\beta(n_t) = J n_t - \alpha_\tau^0 = (J_W + \alpha_\tau^0) n_t - \alpha_\tau^0, \quad (45)$$

where in the last step we have anticipated the relation between J and J_W discussed below (eq. (47)). As already mentioned the numerical value of α_τ^0 may not coincide with the one found by Karsch in [20] and reported in sec. 2.1, as the contributions of the space-like plaquettes have not been taken into account here. The value of α_τ^0 is calculated in this context in sec. 6.1 and it turns out to be close to the one calculated in [20] including the space-like plaquettes. In the strong coupling regime by using eq. (26) we find

$$J_W = 2 \left(\frac{\beta(n_t)}{2} \right)^{n_t}. \quad (46)$$

Let us stress again that both eq. (46) and the linear scaling in the weak coupling regime must be considered as asymptotic behaviours, while eq. (44) for the heat kernel action is exact. It is useful to write explicitly the relation between the normalized couplings J_W and J . They can be found immediately by setting $n_t = 1$ in (40) in the weak coupling and from (43) in the strong coupling. In the weak coupling regime we have

$$J_W = J - \alpha_\tau^0, \quad (47)$$

and in the strong coupling

$$J_W = 2 e^{-\frac{1}{2J}} + \dots. \quad (48)$$

The important lesson that we learn from this analysis is that in the continuum limit all these actions obey a *linear* scaling law. Notice that this scaling behaviour does not depend on the number of spatial dimensions d of the model. This is clearly an artifact of our approximation, and a quite disappointing one, since we know very well that the scaling laws do indeed depend on d . The situation is somehow reminiscent of what happens in the case of the mean field approximation. However, while in the case of mean field we know that the approximation becomes better and better as d increases, here the situation is exactly reverted, and the approximation that we make by neglecting the space-like plaquettes becomes worse and worse as d increases. As a matter of fact this linear scaling agrees with what we expect for the (2+1) dimensional gauge models, but disagrees with our expectations in the (3+1) dimensional case.

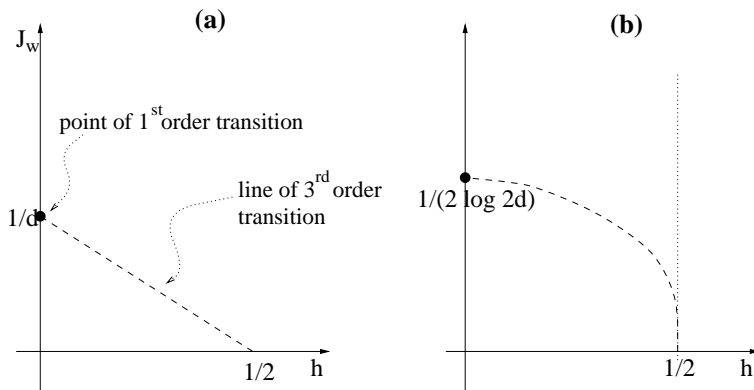


Fig. 2: (a) Phase diagram resulting from the large N limit of the effective model eq.(50); (b) The same diagram expressed in terms of the heat kernel coupling J (related to the Wilson one by $J_W = 2 \exp\{-1/(2J)\}$, see sec. 3.1.3, eq. (48)).

3.1.4 A simplified effective action

It is instructive, before analysing the rather complex model given in (41), to study the simplified effective action which is obtained from the Wilson one, eq. (42), by truncating the character expansion to the lowest order term:

$$S_{\text{eff}}(J_W) = \sum_{\vec{x}} \text{Re} \left\{ J_W \sum_i (\hat{P}(\vec{x}))(\hat{P}^\dagger(\vec{x} + \hat{i})) \right\}. \quad (49)$$

This model is a rather crude approximation of the original action. Due to the truncation, it does not even treat exactly the timelike part of the action, so it cannot be trusted in the weak coupling regime or in the $\rho \rightarrow \infty$ limit where all the terms in the character expansion become important. However this model is very simple to study, it can be easily solved exactly and for this reason it has been very popular in the past years. It was extensively studied in the literature, both at finite N [27, 28] and in the large N limit [29, 30], with strong coupling [31, 32] and mean field [28] approximations, and with Montecarlo simulations [28, 33]. Notwithstanding its simplicity it turned out to be a valuable tool to understand the general features of the phase diagram. Its exact solution in the large N limit was derived in [29, 30], for any value of the space dimensions d , leading to a phase diagram with a first order deconfinement transition located at $J_W = 1/d$. It is even possible to solve exactly the more general model in which the Polyakov loop is also coupled to an external “magnetic” field h ,

$$S_{\text{eff}}(J_W, h) = \sum_{\vec{x}} \text{Re} \left\{ J_W \sum_i \text{Tr}(P(\vec{x}))\text{Tr}(P^\dagger(\vec{x} + \hat{i})) \right\} + hN \sum_{\vec{x}} [\text{Tr}(P(\vec{x}) + P^\dagger(\vec{x}))]. \quad (50)$$

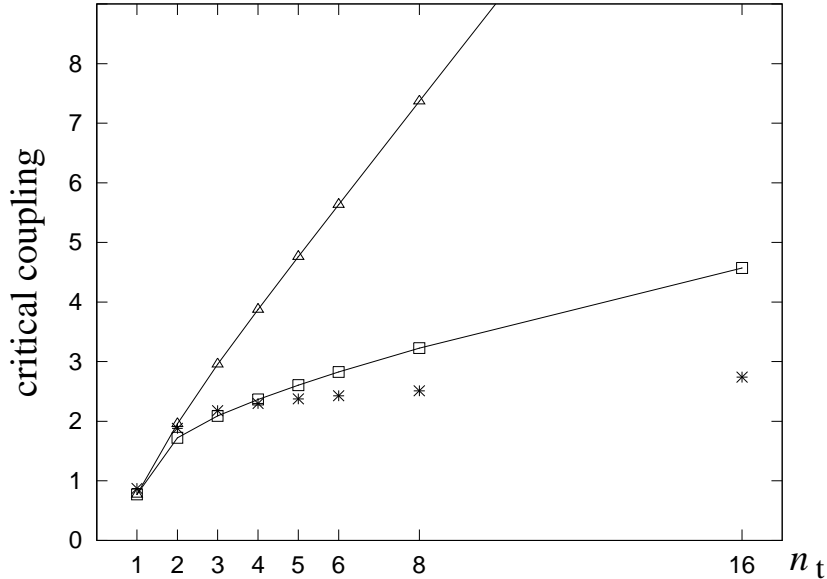


Fig. 3: Values of the critical coupling β_c in the $SU(2)$ theory are plotted for different values of the number of time-like links n_t . Results obtained with Montecarlo simulations, which are denoted by *, are compared with those obtained in [26]: Δ represents the data for $\beta_c|_0$, the critical coupling in the zeroth order approximation and \square the data for $\beta_c|_1$, the critical coupling including the effect of the space-like plaquettes at the lowest non trivial order.

In this framework it becomes apparent that the first order phase transition is the end point of a line of third order phase transitions of the Gross–Witten [34] type, located along the line

$$J_W = \frac{1 - 2h}{d}, \quad h, J_W \geq 0. \quad (51)$$

As we shall see below, keeping the whole complexity of the heat kernel (or Wilson) effective action, the phase diagram turns out to be more rich and complex and also the location of the deconfinement transition changes. In particular in sec. 5.3 we shall discuss the phase diagram of the Wilson action coupled to a “magnetic” field h as in eq. (50) up to the second order in the strong coupling expansion.

3.2 Toward an exact dimensional reduction

3.2.1 Higher orders in β_s

We have seen in the previous subsections that the naive (zeroth order) effective actions fails to catch the correct scaling behaviour of the theory. Our hope is that we can overcome this problem by taking into account higher order contributions in β_s . In [26] we tested this expectation in the case of the $SU(2)$ model in (3+1) dimensions and found a remarkable improvement in the scaling behaviour of the model by adding the terms of order β_s^2 . This is well summarized in Fig. 3 where the two scaling behaviours of the zeroth order and of the β_s^2 order actions are compared with the results of the Montecarlo simulations.

A similar analysis in the large N limit is still missing. In this subsection we shall give some preliminary result in this direction and in particular we shall show that, at least, the problem is well defined and higher order contributions do not diverge as $N \rightarrow \infty$.

The expansion in powers of β_s of the full partition function (34) can be formally written as:

$$e^{S_{\text{Pol}}} = e^{S_{\text{Pol}}(\beta_s=0)} \left\{ 1 + N^2 \beta_s \sum_{\vec{x}, t} \sum_{i < j} \langle G_{ij}(\vec{x}, t) \rangle + \frac{1}{2} N^4 \beta_s^2 \sum_{\vec{x}_1, t_1} \sum_{\vec{x}_2, t_2} \sum_{i_1 < j_1} \sum_{i_2 < j_2} \langle G_{i_1 j_1}(\vec{x}_1, t_1) G_{i_2 j_2}(\vec{x}_2, t_2) \rangle + \dots \right\} \quad (52)$$

where the expectation values are taken with respect to the unperturbed action, namely with $\beta_s = 0$. The series in brackets at the r.h.s. of eq. (52) can be re-exponentiated, leading to the following expansion for S_{Pol} :

$$S_{\text{Pol}} = S_{\text{Pol}}(\beta_s = 0) + N^2 \beta_s \sum_{\vec{x}, t} \sum_{i < j} \langle G_{ij}(\vec{x}, t) \rangle_c + \frac{1}{2} N^4 \beta_s^2 \sum_{\vec{x}_1, t_1} \sum_{\vec{x}_2, t_2} \sum_{i_1 < j_1} \sum_{i_2 < j_2} \langle G_{i_1 j_1}(\vec{x}_1, t_1) G_{i_2 j_2}(\vec{x}_2, t_2) \rangle_c + \dots, \quad (53)$$

where the subscript c denotes the connected part, for instance

$$\langle G_1 G_2 \rangle_c = \langle G_1 G_2 \rangle - \langle G_1 \rangle \langle G_2 \rangle.$$

A few remarks about the general structure of this perturbative expansion are in order here: first it should be noticed that according to a general counting [3] of the powers of N in the large N limit we have $\langle G_1 G_2 \dots G_k \rangle_c = O(\frac{1}{N^{2k-2}})$, so that all the terms in the exponent at the l.h.s of (53) are of the same order N^2 . Secondly, each term of order β_s^k involves the expectation value of k space-like plaquettes, and a sum over all their possible space-time positions. If we compare different regularizations, corresponding to different values of ρ , the sum over the time positions of the plaquettes is of order ρ^k while β_s^k rescales like ρ^{-k} . So, although $\beta_s \rightarrow 0$ as $\rho \rightarrow \infty$, the effective coupling of our expansion does not vanish and it coincides with $\beta + \alpha_\sigma^0$ (see eq. (10)). Indeed, as β is the coupling of the symmetric regularization, it is known from asymptotic freedom to grow logarithmically with n_t as the continuum limit is approached.

It is easy to see that the terms of order β_s in (53) vanish identically and that at the order β_s^2 the only surviving contributions come from two space-like plaquettes in the same space position and separated by an arbitrary time interval. These type of contributions were explicitly calculated in the case of a gauge group $\text{SU}(2)$ in Ref. [26]; for an arbitrary N the calculation up to order β_s^2 has not been done yet and it would involve the explicit evaluation of an integral of the type

$$\int DU D\tilde{U} U_{\alpha\beta} \tilde{U}_{\gamma\delta}^\dagger \chi_r(U\tilde{U}^\dagger) \chi_s(\tilde{U}\Omega_1 U^\dagger \Omega_2^\dagger). \quad (54)$$

This could be done by resorting to the same techniques (use of suitable Schwinger-Dyson equation) used in the $SU(2)$ case [26].

3.2.2 Eguchi–Kawai approach

In the present section we shall derive an exact dimensional reduction to $N_t = 1$. This can be achieved by using ideas similar to the ones used to reduce in the large N limit lattice gauge theories to twisted⁶ one plaquette models. This idea was first proposed by Eguchi and Kawai [6] and subsequently perfected by several authors and it is based on the observation that in the large N limit a suitably twisted lattice gauge theory on a lattice consisting of just one site and one link variable for each space-time direction generates the same set of loop equations as a theory defined on a large lattice, typically consisting of $N^{(d+1)/2}$ sites. Hence twisted one plaquette models can be used to describe lattice gauge theories on large lattices, by essentially mapping space-time degrees of freedom into internal degrees of freedom. A general review of the Eguchi–Kawai model, including applications to finite temperature lattice gauge theories, can be found in [3]. Following [18], rather than applying directly the Eguchi–Kawai method, we shall use a similar technique to reduce to one the size of the lattice only in the compactified time dimension. The fact that such exact dimensional reduction is possible is in itself an interesting result. In sec. 6.1 we shall solve the model in the zeroth order approximation ($\beta_s = 0$) by assuming as usual that the master field is invariant under translations in space. In this limit the final result is the same that one would obtain with a standard hot twisted Eguchi–Kawai model, where the dimensional reduction is done at the same time in all space-time direction. The present approach however has the advantage of being consistent in any space-time dimension, while the Eguchi–Kawai reduction only works for even dimensions. This will allow us to apply it in the case of (2+1) dimensions.

Let us consider again the Wilson action given in eq. (2). A naive prescription for the reduction of the degrees of freedom in the time direction would be

$$\begin{aligned} V(\vec{x}, t) &\rightarrow V(\vec{x}) , \\ U_i(\vec{x}, t) &\rightarrow U_i(\vec{x}) . \end{aligned} \tag{55}$$

Let us denote with $S_W(N_t = 1)$ the action resulting from (2) with the substitution (55). It is easy to show by standard methods (see for instance [3]) that $S_W(N_t = 1)$ leads to the same set of loop equations in the large N limit as the full S_W theory, *provided all loops which are closed in the reduced lattice ($N_t = 1$) but correspond to open loops in the original lattice have vanishing expectation value*. This would be granted by the fact that, in addition to local gauge invariance, $S_W(N_t = 1)$ is endowed with the symmetry

$$V(\vec{x}) \rightarrow e^{i\frac{2\pi n}{N}} V(\vec{x}) \tag{56}$$

⁶The twist consists in a suitable phase factor belonging to the center of $SU(N)$ that multiplies each plaquette variable in the action.

The trace along “open” lines is not invariant under the symmetry (56) as they do not contain the same number of $V(\vec{x})$ and $V^\dagger(\vec{x})$ fields. So these contributions vanish unless the symmetry is broken. The symmetry however is actually broken in the weak coupling regime, that is also in the continuum limit, where $V(\vec{x})$ is close to $\mathbf{1}$ (more generically to an element of \mathbf{Z}_N) and the traces of open lines do not vanish. Consequently the reduction prescription must be modified, as in the twisted Eguchi–Kawai model, according to the formula:

$$\begin{aligned} V(\vec{x}, t) &\rightarrow D(\vec{x}, t)V(\vec{x})D^\dagger(\vec{x}, t) , \\ U_i(\vec{x}, t) &\rightarrow D(\vec{x}, t)U_i(\vec{x})D^\dagger(\vec{x}, t) , \end{aligned} \quad (57)$$

where $D(\vec{x}, t)$ is given by

$$D(\vec{x}, t) = (\Gamma) \sum^{x_i} (\Gamma_0)^t , \quad (58)$$

with Γ and Γ_0 traceless $\text{SU}(N)$ matrices satisfying the 't Hooft algebra

$$\Gamma\Gamma_0 = e^{i\frac{2\pi}{N}m}\Gamma_0\Gamma . \quad (59)$$

In the last equation m is an integer number to be determined. By performing in the Wilson action (2) the replacement (57) and redefining the variables according to the substitution $U_i(\vec{x}) \rightarrow U_i(\vec{x})\Gamma$ and $V(\vec{x}) \rightarrow V(\vec{x})\Gamma_0$ we obtain the “reduced” partition function

$$\begin{aligned} Z_{\text{red}} &= \int \prod_{\vec{x}} [DV(\vec{x}) \prod_{i=1}^d DU_i(\vec{x})] \exp(S_R) , \\ S_{\text{red}} &= \beta_t N \sum_{\vec{x}} \sum_{i=1}^d \text{Re} e^{i\frac{2\pi m}{N}} \text{Tr}[U_i(\vec{x})V(\vec{x} + \hat{i})U_i^\dagger(\vec{x})V^\dagger(\vec{x})] + \\ &\quad \beta_s N \sum_{\vec{x}} \sum_{i>j} \text{Re} \text{Tr}[U_i(\vec{x})U_j(\vec{x} + \hat{i})U_i^\dagger(\vec{x} + \hat{j})U_j^\dagger(\vec{x})] . \end{aligned} \quad (60)$$

Notice that, unlike the twisted Eguchi–Kawai model, the twists are present in (60) only in the contributions from time-like plaquettes, as the reduction has been done only in the time direction.

Consider now the loop equations for the reduced theory (60). We already remarked that as long as the symmetry (56) is unbroken the loop equations of the reduced theory coincide with the ones of (2). We will show now that in the twisted theory this is the case *also in the weak coupling regime*. Indeed in the extremely weak coupling the fields tend to their vacuum configurations, which in our twisted reduced theory are

$$\begin{aligned} U_i(\vec{x}) &\rightarrow P_{\frac{N}{m}} \otimes \mathbf{1}_m , \\ V(\vec{x}) &\rightarrow Q_{\frac{N}{m}} \otimes \mathbf{1}_m , \end{aligned} \quad (61)$$

where $\mathbf{1}_m$ is the $m \times m$ unit matrix and $P_{\frac{N}{m}}$ and $Q_{\frac{N}{m}}$ are the usual building blocks for the twist eating configurations:

$$(P)_{ab} = \delta_{a+1,b} \quad ; \quad (Q)_{ab} = \delta_{ab} e^{i\frac{2\pi m}{N}a} \quad , \quad a, b = 1, \dots, N/m \quad (62)$$

with periodicity in the the indices a and b , namely $a = \frac{N}{m} + 1$ means $a = 1$. It is clear from the context that we have to restrict the values of N so that N/m is an integer. With these vacuum configurations the trace of open lines is proportional to $\text{Tr}(Q_{\frac{N}{m}})^t$, where t is the difference between the number of V 's and V^\dagger 's in the trace, namely the difference between the time coordinate of the initial and the final point of the path in original unreduced lattice. It is elementary to see from eq. (62) that

$$\text{Tr}(Q_{\frac{N}{m}})^t = 0 \quad \text{unless} \quad t = k\frac{N}{m} \quad (63)$$

for integer k . In the unreduced lattice closed loops correspond to $t = kN_t$, so the comparison of the two equations determines m :

$$m = \frac{N}{N_t} . \quad (64)$$

With the above replacement eq. (60) is, in the large N limit, an exact dimensional reduction of (2) on a d -dimensional lattice.

4 Phase diagram of the Effective Model

While the exact solution of the effective model for the Polyakov loops given in eq. (52) is well beyond our computational capabilities, its zeroth order approximation in the β_s expansion can be studied and solved analytically, within reliable approximation schemes, in both the weak coupling and the strong coupling regime. In particular, we consider in this section the effective action for the Polyakov loop at $\beta_s = 0$, eq. (41), that is obtained in the $\rho \rightarrow \infty$ limit (heat kernel action), with the aim of describing its phase diagram.

The solution of the model (41) will rely, in both the weak and the strong coupling regime, on the assumption that a translational invariant master field describes the eigenvalue distribution of the Polyakov loop in the large N limit. In the weak coupling region, namely for large $J = \beta_{\text{hk}}(n_t = 1)$, we know that the model is in a deconfined phase where $\hat{P}(\vec{x}) \neq 0$, and the invariant angles of the Polyakov loop are distributed around $\theta = 0$. The solution of model can then be obtained by retaining only quadratic fluctuations of the eigenvalues around $\theta = 0$. This is done in subsection 4.1, where it is shown that the model obtained from this quadratic approximation is a solvable model of the type known as ‘‘Kazakov–Migdal model’’ [14]. The solution is a semicircular distribution of eigenvalues, centered around $\theta = 0$, with a radius that increases as J decreases and acquires an imaginary part at a critical value of J . As first noticed by Zarembo in [16], this denotes an instability

of the weak coupling solution and puts a lower bound for a phase transition. A deeper insight into the meaning of this phase transition, as well as a more accurate determination of the critical value of J , is obtained in subsection 4.1.2 following the remark that the contribution to the action (41) from any pair of nearest neighbour Polyakov loops is exactly the action of QCD2 on a cylinder, of area $\frac{1}{J}$ and with the holonomies at the ends of the cylinder coinciding with the open Polyakov loops. When the holonomies at the boundaries are given by semicircular distributions of eigenvalues, as in the quadratic approximation mentioned above, QCD2 on a cylinder can be solved exactly and it is known to have a third order phase transition [40], as Douglas and Kazakov [35] first discovered in the case of a sphere, due to the condensation of instantons. In the present context this not only clarifies the nature of the phase transition but, as already mentioned, increases by a few percent the lower bound already established by Zarembo's argument. The strong coupling regime is studied in subsec. 4.2. In this phase (small J) the vacuum is symmetric, $\hat{P}(\vec{x}) = 0$, namely it is characterised by a uniform distribution of eigenvalues. Two types of results can be obtained in this context. A strong-coupling expansion of the effective model (that was pushed up to the 4th order in [15]) shows that a new maximum, other than the symmetric one, appears as J increases, it becomes competitive with the symmetric one at a critical coupling J_c and it is energetically favoured for $J > J_c$. We have therefore, at $J = J_c$, a 1st order transition. It is also possible [16] to calculate exactly, namely at all orders in J , the mass of the lowest excitation in the fluctuations around the symmetric vacuum, and hence to calculate exactly for which value of J the symmetric vacuum becomes unstable. This argument determines an upper bound for the critical value of J , which, at least for not too high values of the number d of space dimensions, is higher than the lower bound determined by the weak coupling analysis, thus restricting to a rather narrow band the region in which the deconfinement transition must take place.

4.1 Weak coupling expansion

The building block of the partition function (41), that is the contribution of two nearest neighbour Polyakov loops, is given by a kernel of the form:

$$\mathcal{K}_2(g_1, g_2; \mathcal{A}) = \sum_r \chi_r(\phi) \chi_r(\theta) e^{-\frac{C_r \mathcal{A}}{2N}} , \quad (65)$$

where ϕ and θ denote the invariant angles respectively of g_1 and g_2 . It is well known (see for instance [9, 8]) that $\mathcal{K}_2(g_1, g_2; \mathcal{A})$ is the partition function of QCD2 on a cylinder of area \mathcal{A} and boundary holonomies g_1 and g_2 . With this notation the partition function (41) can be rewritten as

$$Z = \int \prod_{\vec{x}} DP(\vec{x}) \prod_{\vec{x}, i} \mathcal{K}_2(P(\vec{x}), P(\vec{x} + i); 1/J), \quad (66)$$

where J is the “renormalized” coupling $J = \beta_t(N_t = 1)$ introduced in eq. (44).

In the large N limit we can assume that the saddle point solution is translational invariant and, as a consequence, the action reduces to a one plaquette integral. The partition function is then simply given by

$$Z = \int DP [\mathcal{K}_2(P, P^\dagger; 1/J)]^d, \quad (67)$$

where d is the number of space dimensions. Solving the model amounts to finding the eigenvalue distribution $\rho(\theta)$ for the eigenvalues of the Polyakov loop $P = e^{i\theta}$ that is an extreme of the free energy associated with eq. (67). In order to do that let us first rewrite eq. (67) explicitly as an integral over the invariant angles of P . This involves the explicit expression for the characters $\chi(\theta)$ of $SU(N)$:

$$\chi_r(\theta) = \frac{\det \{e^{ir_i\theta_j}\}}{\mathcal{J}(\theta)} (-i)^{N(N-1)/2} \quad (68)$$

where $\mathcal{J}(\theta)$ is the Vandermonde determinant for a unitary matrix,

$$\mathcal{J}(\theta) = \prod_{i<j} 2 \sin \frac{\theta_i - \theta_j}{2}, \quad (69)$$

and the set of integers r_i label the representation r of $SU(N)$. By using eq. (68), the explicit expression of the Casimir C_r , and the Poisson summation formula

$$\sum_{l=-\infty}^{\infty} \exp\left(-\frac{(\theta+l)^2}{4t}\right) = (4\pi t)^{1/2} \sum_{n=-\infty}^{\infty} \exp(-4\pi^2 n^2 t) \exp(2\pi i n \theta), \quad (70)$$

we can rewrite (67) in the following way⁷:

$$Z = \int \prod d\theta_i [\mathcal{J}^2(\theta)]^{(1-d)} \left[\sum_{l_i} \sum_P (-1)^{\sigma(P)} e^{-\frac{1}{2}NJ \sum_i (\theta_i - \theta_{P(i)} + 2\pi l_i)^2} \right]^d. \quad (71)$$

where P denotes a permutation (of signature $\sigma(P)$) of the indices. The r.h.s. of (71) depends upon a new set of integers l_i , which are the winding numbers of the eigenvalues on the unit circle⁸. In the weak coupling (large J) regime, we can assume that the invariant angles θ_i are small and that the contributions of the winding (i.e. $l_i \neq 0$) configurations, which are exponentially depressed, can be neglected. We shall actually prove in the next section that in the large N limit and

⁷The calculation is almost straightforward in the case of $U(N)$ where the sum over the integers r_i is unrestricted and the Casimir is simply given by $C_r = \sum_i r_i^2$. The details of the calculation in the $SU(N)$ case can be found in [36].

⁸Similarly the integers r_i labelling the representations can be interpreted as discretized momenta, and the Poisson summation formula as the corresponding discrete Fourier transform. This will be further clarified in the next section 4.1.2.

above a critical value of J the vanishing of the contributions of the winding modes is an exact result. Hence we set $l_i = 0$ in eq. (71). Moreover, for small θ we have

$$\mathcal{J}^2(\theta) = \Delta^2(\theta) e^{-\frac{1}{12}N \sum_i \theta_i^2 + O(\theta^4)}, \quad (72)$$

where $\Delta(\theta) = \prod_{i < j} (\theta_i - \theta_j)$ is the usual Cauchy–Vandermonde determinant. Inserting these results in eq. (71) we obtain

$$\int \prod_i d\theta_i \left[\Delta^2(\theta) \right]^{(1-d)} e^{-N[dJ - \frac{d-1}{12}] \sum_i \theta_i^2} \left[\sum_P (-1)^{\sigma(P)} e^{NJ\theta_i \theta_{P(i)}} \right]^d. \quad (73)$$

Notice that, provided J is larger than its critical value, the only approximation needed to go from eq. (67) to eq. (73) consists in neglecting the $O(\theta^4)$ terms in (72).

4.1.1 Solution via the Kazakov–Migdal model

The model given in (73) coincides with a Kazakov–Migdal (KM) matrix model with quadratic potential, which is exactly solvable.

The KM model [14] can be defined, in its discretized version, by the following partition function on a d -dimensional hypercubic lattice:

$$Z_{KM} = \int \prod_{\vec{x}} D\phi(\vec{x}) \prod_{\vec{x}, i} DU_i(\vec{x}) \times \exp \left\{ \sum_{\vec{x}} N \text{Tr} \left(-V(\phi(\vec{x})) + \sum_{i=1}^d \phi(\vec{x}) U_i(\vec{x}) \phi(\vec{x} + \hat{i}) U_i^\dagger(\vec{x}) \right) \right\}, \quad (74)$$

where $\phi(\vec{x})$ is an Hermitian $N \times N$ matrix and the link matrices $U_i(\vec{x})$ belong to $SU(N)$. $V(\phi)$ is a potential term.

While the model (74) contains no self-interaction between the “gauge” fields $U_i(\vec{x})$, if one integrates out the $\phi(\vec{x})$ fields the resulting effective model for the gauge fields (known as “induced gauge model”) includes peculiar gauge self-interactions. The original hope that the induced gauge model could describe directly QCD in d dimensions was however shown to fail [37] due to the super-confining behaviour of the former.

Another way to deal with eq. (74) is to carry out first the integration over the link matrices, to obtain an effective model for the $\phi(\vec{x})$ ’s. To do so, one utilizes typical matrix model techniques. First the gauge is fixed so that the ϕ ’s are diagonal:

$$\begin{aligned} \phi(\vec{x})_b^a &\rightarrow \delta_b^a \lambda_a(\vec{x}) \\ D\phi(\vec{x}) &\rightarrow \left[\prod_a d\lambda_a(\vec{x}) \right] \Delta^2(\lambda). \end{aligned} \quad (75)$$

Then the integration over the links is carried out utilizing the Harish–Chandra–Itzykson–Zuber–Mehta integral [38]:

$$\int DU_i(\vec{x}) e^{N \text{Tr} U_i(\vec{x}) \lambda(\vec{x}+i) U_i^\dagger(\vec{x}) \lambda(\vec{x})} = \sum_P (-1)^P \frac{e^{N \sum_a \lambda_a(\vec{x}) \lambda_{Pa}(\vec{x}+i)}}{\Delta(\lambda(\vec{x})) \Delta(\lambda(\vec{x}+i))}. \quad (76)$$

For a quadratic potential $V(\phi(\vec{x})) = \frac{1}{2} m^2 \phi^2(\vec{x})$, and in the large N limit, in which one looks for a translationally invariant master field $\lambda_a(\vec{x}) \rightarrow \lambda_a$, the resulting model is:

$$Z_{KM} = \int \prod_a d\lambda [\Delta^2(\lambda)]^{1-d} e^{-N \frac{m^2}{2} \sum_a \lambda_a^2} \left[\sum_P (-1)^{\sigma(P)} e^{N \sum_a \lambda_a \lambda_{Pa}} \right]^d. \quad (77)$$

Gross [19] found the master field that *exactly* solves, for any d , this model to be given by a semicircular Wigner eigenvalue distribution:

$$\rho(\lambda) = \frac{2}{\pi R^2} \sqrt{R^2 - \lambda^2}, \quad (78)$$

where the radius R is given by

$$R^2 = \frac{4(2d-1)}{(m^2(d-1) + d\sqrt{m^4 - 4(2d-1)})}. \quad (79)$$

This exact solution provides us, as we shall see in a moment, with the solution for the small- θ expression eq. (73) of our effective model.

Let us still remark that, although unsuitable for the description of QCD in d dimensions, the d -dimensional KM model was soon argued to be related with finite-temperature QCD in $d+1$ dimensions [39]. Indeed the presence of “matter” fields $\phi(\vec{x})$ in the adjoint representation of the gauge group led to conjecture that they could be the remnants of the components of the gauge fields in an extra compactified direction. This extra dimension is naturally interpreted as the time-like direction in a finite-temperature model.

Going back to our effective model for the Polyakov loops, given, in the approximation of small eigenvalues, by eq. (73), and comparing it with eq. (77), we see that indeed it is a quadratic KM model⁹ with mass

$$m^2 = 2d - \frac{d-1}{6J}. \quad (80)$$

The solution of the our model, which is exact as long as eq. (73) is exact, i.e. as long as quartic and higher terms in the θ 's are negligible, is therefore given by a Wigner distribution $\rho(\theta)$ of radius

$$r^2 = \frac{4(2d-1)}{J(m^2(d-1) + d\sqrt{m^4 - 4(2d-1)})}. \quad (81)$$

⁹The overall factor of J in the exponent in eq. (73) amounts just to a different normalization of the θ 's.

The radius of the distribution depends on the coupling J (a part from the overall factor of $\frac{1}{J}$) through the expression (80) of the mass.

Because of the dependence of m^2 from the coupling J , it is easy to see that the argument of the square root in (81) decreases as J decreases, and it eventually becomes negative. Correspondingly the radius r^2 of the distribution acquires an imaginary part, thus making the solution of our model inconsistent. It was argued in [16] that this is a signal that the weak coupling solution becomes instable and that we are in presence of a phase transition. The corresponding values of J , for various dimensions d , are reported in the last column of Tab. I at the end of the following section.

A deeper insight of this phase transition will be obtained in the next section, following the identification of $\mathcal{K}_2(g_1, g_2; \mathcal{A})$ with the action of QCD2 on a cylinder. We just remark here that in the present calculation the instability of the weak coupling solution stems from the J -dependence of m^2 , namely from the fact that the Vandermonde determinant $\mathcal{J}^2(\theta)$ for unitary matrices appears in eq. (71) instead of the usual Vandermonde determinant $\Delta^2(\theta)$. So, in spite of neglecting the winding modes l_i , our solution “knows” that the eigenvalues live on a circle rather than on a line and that the excitation of the winding modes becomes eventually favourite, thus leading to a phase transition.

4.1.2 Douglas–Kazakov phase transition on a cylinder

We have already remarked that the kernel $\mathcal{K}_2(g_1, g_2; \mathcal{A})$ defined in (65) is the partition function of QCD2 on a cylinder of fixed area and boundary holonomies. The fact that it appears as the basic ingredient in our effective action at $\beta_s = 0$ is not really a surprise, as the space-like plaquettes are absent in $d = 1$ and $\beta_s = 0$ is exact in that case. So, in order to compute the partition function of QCD2 on a cylinder we can use a heat kernel regularization and start from eq. (34) with $\beta_s = 0$. The different steps of the calculation are depicted in Fig. 4, and correspond the the steps leading from eq. (34) with $\beta_s = 0$ to eq. (41) but with the additional integration over all intermediate timelike links. The final integration over the remaining space-like link leads to the r.h.s of (41), but with the space lattice consisting just of the two end points of the cylinder, and with the area appearing in the exponent. This is exactly $\mathcal{K}_2(g_1, g_2; \mathcal{A})$. The partition function of QCD2, not just on a cylinder but on a generic space-time manifold is known exactly, and it has been extensively studied. It was soon recognised by Douglas and Kazakov [35] that in QCD2 on a sphere a third order phase transition occurs at a critical value of the area. This result was later generalized to the case of a cylinder [40, 15, 10, 11] and the corresponding phase transition will therefore be called in the following “Douglas–Kazakov (DK) phase transition on a cylinder”. In order to study this transition let us first rewrite $\mathcal{K}_2(g_1, g_2; \mathcal{A})$ by using the Poisson summation formula (70). The result is [41, 36]:

$$\mathcal{K}_2(g_1, g_2; \mathcal{A}) = \left(\frac{N}{4\pi}\right)^{1/2} \exp\left(\frac{\mathcal{A}}{24}(N^2 - 1)\right) \sum_P \frac{(\frac{\mathcal{A}}{N})^{(1-N)/2}}{\mathcal{J}(\theta)\mathcal{J}(\phi)} \quad (82)$$

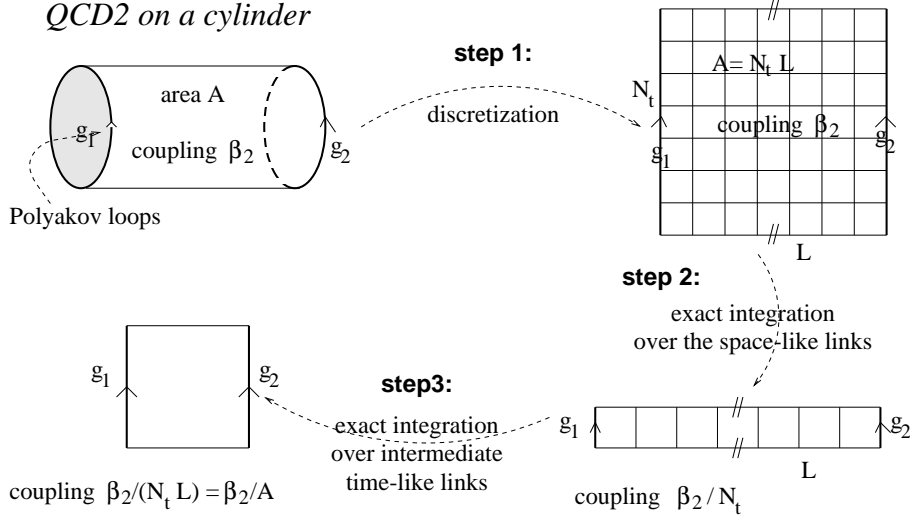


Fig. 4: The partition function of the QCD2 on the cylinder can be derived exactly via discretization. See the text for explanation.

$$(-1)^{\sigma(P)} \sum_{\{l_i\}} \exp \left[-\frac{N}{2\mathcal{A}} \sum_{i=1}^N (\phi_i - \theta_{P(i)} + 2\pi l_i)^2 \right],$$

where as usual P denotes a permutation of the indices. It is easy to check directly on (82) that $\mathcal{K}_2(g_1, g_2; \mathcal{A})$ is the solution of the heat kernel equation on the $SU(N)$ group manifold

$$\left(N \frac{\partial}{\partial \mathcal{A}} - \frac{1}{2} \mathcal{J}^{-1}(\phi) \sum_i \frac{\partial^2}{\partial \phi_i^2} \mathcal{J}(\phi) - \frac{1}{24} N(N^2 - 1) \right) \mathcal{K}_2(\phi, \theta; \mathcal{A}) = 0 \quad (83)$$

uniquely determined by the condition

$$\lim_{\mathcal{A} \rightarrow 0} \mathcal{K}_2(g_1, g_2; \mathcal{A}) = \hat{\delta}(g_1, g_2), \quad (84)$$

where, in the notations of Ref. [36], $\hat{\delta}$ is the invariant delta function on the group manifold. As pointed out in [36, 42], redefining the Kernel by $\mathcal{K}_2(\phi, \theta; \mathcal{A}) \rightarrow \hat{\mathcal{K}}_2 = \mathcal{J}(\phi) \mathcal{J}(\theta) \mathcal{K}_2$, eq. (83) becomes the (Euclidean) free Schroedinger equation for N fermions on a circle, where \mathcal{A} plays the role of (Euclidean) time. This means that, because of the condition (84), we can interpret $\mathcal{K}_2(\phi, \theta; \mathcal{A})$ as the Euclidean transition amplitude for this system of fermions, from the configuration $\{\phi_i\}$ at zero time to the configuration $\{\theta_i\}$ at the time \mathcal{A} . The modular transformation eq. (70), relating eq. (82) to eq. 65, admits a straightforward interpretation in the fermionic language: the integers labelling the unitary representations in the character expansion (65) correspond to discretized momenta of the fermions on the circle, while eq. (82) gives the corresponding coordinate representation, and the integers in the co-root lattice are the fermion winding numbers.

The expressions (65,82) of the kernel depend upon two sets of eigenvalues, $\{\phi_i\}$ and $\{\theta_i\}$. The specific eigenvalues do not tend to any limit as N goes to infinity; however, the corresponding eigenvalue distributions¹⁰ do have a large N limit, and contain all the information needed to evaluate the large N asymptotics of \mathcal{K}_2 .

In particular, it is possible to write, in the large N limit, the time evolution equation (83) as a functional differential equation for the smooth functional of the eigenvalue densities $F[\rho_0, \rho_1; \mathcal{A}]$, defined as $\mathcal{K}_2(\phi, \theta; \mathcal{A}) = \exp(N^2 F[\rho_0, \rho_1; \mathcal{A}])$, ρ_0 and ρ_1 being the densities corresponding to $\{\phi\}$ and $\{\theta\}$ respectively. This goal is achieved by replacing partial derivatives in (83) by derivatives with respect to the eigenvalue densities,

$$N \frac{\partial F}{\partial \phi} = \frac{\partial}{\partial x} \left. \frac{\delta F}{\delta \rho(x)} \right|_{x=\phi_i}, \quad (85)$$

and all sums by integrals (see Ref. [43] for the details of the calculation). The final result [43, 15, 16] is that the time (area) evolution of the eigenvalue distribution $\rho(x)$ is governed, at the leading order in $1/N$, by a Das–Jevicki Hamiltonian [44],

$$H[\rho(x), \Pi(x)] = \frac{1}{2} \int dx \rho(x) \left\{ \left(\frac{\partial \Pi(x)}{\partial x} \right)^2 - \frac{\pi^2}{3} \rho^2(x) \right\}, \quad (86)$$

where $\Pi(x)$ is the canonical momentum conjugate to $\rho(x)$. In terms of the complex quantity

$$f(x, t) = \frac{\partial \Pi(x, t)}{\partial x} + i\pi \rho(x, t) \quad (87)$$

the equation of motion becomes the Hopf equation for an ideal fluid,

$$\frac{\partial f}{\partial t} + f \frac{\partial}{\partial x} f = 0, \quad (88)$$

with the boundary conditions

$$\rho(x, t = 0) = \pi \rho_0(x), \quad \rho(x, t = \mathcal{A}) = \pi \rho_1(x). \quad (89)$$

The solutions to the equations (88,89) have been studied in detail by Gross and Matytsin [11]. The knowledge of these solutions allows to write the *exact* expression, in the large N limit, of the free energy corresponding to the partition function (65). The free energy exhibits a 3rd order phase transition, for a critical value \mathcal{A}_c of the area [i.e. of the coupling] that we shall derive in a moment. This transition is the exact analogue of the 3rd order transition of QCD2 on the sphere, discovered by Douglas and Kazakov [35]; actually the case of the sphere is retrieved when the boundary distributions both degenerate to delta functions.

¹⁰If $\{\phi_i\}$ is a set of invariant angles, the corresponding distribution is defined as $\rho(x) = \frac{1}{N} \sum_i \delta(x - \phi_i)$. Notice that distributions corresponding to set of angles are periodic functions of x , with period 2π .

For our purposes it is sufficient to follow the derivation first given in [40] of the critical value \mathcal{A}_c . In order to find a solution to the eq.s (88,89) consider the ansatz corresponding to a semicircular Wigner distribution of variable radius,

$$\begin{aligned}\rho(x, t) &= \frac{2}{\pi r^2(t)} \sqrt{r^2(t) - x^2}, & |x| < r^2(t) \\ \rho(x, t) &= 0, & r^2(t) < |x| < \pi.\end{aligned}\tag{90}$$

By inserting this ansatz into the Hopf equation we find that it gives a solution of the equation provided the time dependence of the radius r of the distribution is of the form

$$r(t) = 2\sqrt{\frac{(t + \alpha)(\beta - t)}{\alpha + \beta}}.\tag{91}$$

The arbitrary constants α, β are determined by the boundary conditions (89). For consistency, the initial and final distributions in (89) must be semicircular. with radii given by $r(0) = r_0, r(\mathcal{A}) = r_1$. Given r_0 and r_1 , the radius of the distribution is determined at any time along the cylinder by eq. (91). However, because of the periodicity condition on the eigenvalue distribution, the density (90,91) is a solution of the saddle-point equations (88,89) only if $r(t) < \pi$ for any t on the trajectory. For any given value of r_0 and r_1 , the maximum value of $r(t)$ increases as the area \mathcal{A} increases, so the solution (88,91) is valid only if the area \mathcal{A} is smaller than a critical value \mathcal{A}_c , where the maximum radius equals π and the eigenvalues fill up the whole circle. The critical value of \mathcal{A} at which the transition occurs can be easily calculated and is given in [15]. It will be relevant in the following only the case in which $r_0 = r_1 \equiv r$; then

$$(\mathcal{A}_c)^2 = \pi^4 - \pi^2 r^2.\tag{92}$$

Notice that for $r = 0$ the partition function of QCD on a sphere is retrieved. Consistently, the critical value (92) becomes $\mathcal{A}_c = \pi^2$, which is just the value found by Douglas and Kazakov [35].

From the previous discussion one can deduce that below the critical area \mathcal{A}_c the eigenvalue distribution is confined in an interval $(-a(t), a(t))$ with $a(t) < \pi$ for any value of t . Hence the configurations in which a fraction of the eigenvalues wind around the circle do not contribute in the large N limit and all the integers l_i in eq. (82) can be set to zero. The topologically non trivial configurations¹¹ are relevant only if at some value of t the distribution covers the whole unit circle. The role of instantons in inducing the Douglas–Kazakov phase transition on the sphere was fully investigated by Gross and Matytsin [10, 11].

A pictorial view of the DK phase transition is given in Fig. 5.

In order to apply these results to the effective action for the Polyakov loop all we have to do is to remember that the role of the area is played by $1/J$ and that

¹¹These configurations are instantons in the interpretation of the eigenvalues as fermions and of the area as time evolution parameter.

Table I: Value of J below which the Wigner distribution becomes unstable, from the Douglas–Kazakov phase transition (third column) and from Ref. [16]. The radius of the distribution at the critical point is given in the second column.

d	r_c	$J_c^{(w.c.)}$ [Doug. – Kaz.]	$J_c^{(w.c.)}$ [Zarembo]
2	2.96	0.321	0.311
3	2.80	0.226	0.218
4	2.66	0.192	0.184
∞	0.	$1/\pi^2 \sim 0.101$	$1/12 \sim 0.083$

the radius $r(J)$ of the Wigner distribution of the eigenvalues of the Polyakov loop is given by (81). Eq. (92) turns then into an equation for the critical value of J :

$$\left(\frac{1}{J}\right)^2 = \pi^4 - \pi^2 r(J)^2 . \quad (93)$$

This equation can be solved for different values of the number d of space dimensions and the results can be compared with the ones obtained in the previous section by requiring the reality of $r(J)$. The results are summarized in Tab. I. The determination of the critical coupling obtained from the DK phase transition is consistently slightly higher (and hence provides a better lower limit) than the one by Zarembo. On the other hand the two values are very close to each other, thus indicating clearly that we are dealing with the same physical phenomenon, as one could argue from the remark at the end of the previous section, where it was noticed how the radius of the distribution developed an imaginary part at small J as a consequence of the compact and topologically non trivial support (the unit circle) of the eigenvalues of unitary matrices.

The radius of the distribution at the critical DK point, given in the second column of Tab. I, is consistently less than π for any number of dimensions, although very close to it for low dimensions. The same calculation, with the critical J obtained by Zarembo, would instead give a radius larger than π for $d = 2$ and $d = 3$. In spite of the small value of J we expect the weak coupling solution to be very reliable above the DK phase transition, particularly for large d , where the small value of r_c ensures that the quartic terms which have been neglected in eq. (73) are indeed small.

To sum up, we have established that the Wigner distribution of eigenvalues becomes unstable at a value of the coupling constant given by (93), and the transition is driven by the winding modes in the configuration space of the eigenvalues. This analogy with the Douglas–Kazakov phase transition on a sphere gives an almost compelling argument that the corresponding phase transition is of the third order. The appearance at the critical point of new classical trajectories corresponding to winding eigenvalues has presumably the effect of spreading the distribution, especially at the extremes. On the other hand, for low dimensions, the transition occurs

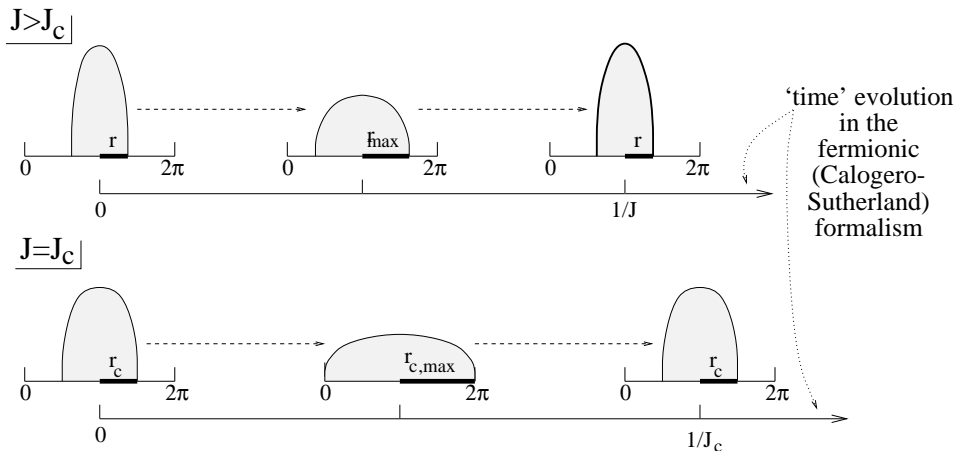


Fig. 5: Mechanism of the Douglas–Kazakov transition, as it applies to our effective model for the Polyakov loops

at a radius of the eigenvalue distribution very near to π . This probably means that the maximum corresponding to the broken, deconfined phase becomes unstable, and the distribution would collapse into the uniform one. However this is not the case for high dimensions, where the critical radius is small, approaching zero as d increases. In this case the Douglas–Kazakov phase transition is a transition from a classical Wigner distribution to another one, so far unknown, but still presumably peaked around the origin. This point will be discussed further in sec. 5.1.

4.2 Strong coupling expansion

Let us turn now our attention to the strong coupling expansion of the effective model (41). In this section, which is mainly based on Ref.s [15, 16, 17], we will pursue this expansion up to the fourth order, obtaining a satisfactory picture of the deconfinement transition as it is seen by approaching the critical value of the coupling J_c from the strong coupling side and also obtaining a rather precise determination of the critical value itself.

We will moreover determine the instability of the strong coupling vacuum (i.e. the point where the uniform eigenvalue distributions turns from a maximum into a saddle point of the effective action); this instability is distinct from the first order deconfinement transition, as will be apparent.

4.2.1 Notations and preliminaries

In the strong coupling region, the vacuum of the theory is the symmetric one: $\langle \hat{P} \rangle = 0$; in terms of the translationally invariant large N solution, it corresponds to a uniform eigenvalue distribution. When J grows and reaches a certain critical

value, a different non-symmetric vacuum, corresponding to a non-uniform eigenvalue distribution, becomes eventually energetically favourable and the transition to the deconfined phase takes place.

The partition function of the model was given in eq. (67), and is repeated here for commodity:

$$Z = \int \prod_i d\theta_i \mathcal{J}^2(\theta) \left[\mathcal{K}_2(P, P^\dagger; 1/J) \right]^d . \quad (94)$$

We are interested in the large N limit. We will therefore search for a “master field” solution, described by a certain eigenvalue distribution, such that it maximizes the free energy that appears in eq. (94). To proceed, we must find the strong coupling expansion in the large N limit of this free energy.

As a preliminary step let us establish some notations. We are interested in the large N limit, so the fundamental quantity is the distribution $\rho(\theta)$ of the eigenvalues of the Polyakov loop. It is convenient to expand $\rho(\theta)$ in its Fourier modes

$$\rho(\theta) = \frac{1}{2\pi} \sum_{n=-\infty}^{\infty} \rho_n e^{in\theta} = \frac{1}{2\pi} \sum_{n=-\infty}^{\infty} x_n e^{i\alpha_n + in\theta} , \quad (95)$$

where $\alpha_n \in (-\pi/2, \pi/2)$ is the argument of ρ_n modulo π , and x_n coincides with the modulus of ρ_n up to a sign¹². The reality of $\rho(\theta)$ requires $\rho_{-n} = \rho_n^*$, while the normalization of $\rho(\theta)$ to 1 in the interval $(-\pi, \pi)$ fixes $\rho_0 = 1$.

The inverse formula

$$\rho_n = \int_{-\pi}^{\pi} \rho(\theta) e^{-in\theta} \quad (96)$$

shows that ρ_n corresponds to the large N limit of the loop winding n times in the time-like direction with the given eigenvalue distribution. In particular, $\rho_{\pm 1}$ corresponds to the large N limit of the Polyakov loop.

The \mathbf{Z}_N invariance of the effective theory becomes, in the large N limit, a $U(1)$ invariance under the shift $\theta \rightarrow \theta + \delta$, that is $\alpha_n \rightarrow \alpha_n + n\delta$. If this symmetry is unbroken the eigenvalue distribution is simply given by $\rho(\theta) = \frac{1}{2\pi}$, namely $x_n = 0$ for $n \neq 0$. In the broken phase the $U(1)$ symmetry connects the different vacua. If we choose the vacuum peaked at $\theta = 0$, then the symmetry of the action for $\theta_i \rightarrow -\theta_i$ will force the vacuum distribution $\rho(\theta)$ to be even in θ , thus fixing all α_n to zero. In this situation the eigenvalue distribution takes the form

$$\rho(\theta) = \frac{1}{2\pi} \left[1 + 2 \sum_{n=1}^{\infty} x_n \cos(n\theta) \right] , \quad (97)$$

with x_n real.

¹²It is convenient for the following discussion to restrict the range for α_n and have x_n taking also negative values.

4.2.2 The integration measure

We need to obtain a strong coupling expansion of the integration measure $\mathcal{J}^2(\theta)$, which in the large N limit can be expressed as a function of the loop variables ρ_n , as

$$\mathcal{J}^2(\theta) = \exp \left[\lim_{y \rightarrow 1} \frac{N^2}{2} \int_{-\pi}^{\pi} d\theta \int_{-\pi}^{\pi} d\varphi \rho(\theta) \rho(\varphi) \log(1 - y \cos(\theta - \varphi)) \right], \quad (98)$$

where the double integral, which would be divergent at $\theta = \varphi$, has been regularized by the inclusion of the parameter y , and terms in the exponent suppressed by powers of N have been neglected. Eq. (98) can be expressed in terms of the modes x_k by expanding in powers of θ and φ and resumming the resulting expression. The result is

$$\mathcal{J}^2(\theta) = \exp \left[\lim_{y \rightarrow 1} N^2 \left(C_0(y) + \sum_{k=1}^{\infty} C_k(y) x_k^2 \right) \right], \quad (99)$$

where $C_0(y)$ is an irrelevant divergent expression and $C_k(y)$ is given by

$$C_k(y) = \frac{1}{k} \left[\frac{1 - \sqrt{1 - y^2}}{y} \right]^k. \quad (100)$$

After removing the divergence, the limit $y \rightarrow 1$ can be taken, and gives

$$\mathcal{J}^2(\theta) = \exp \left[-N^2 \sum_{k=1}^{\infty} \frac{1}{k} x_k^2 \right]. \quad (101)$$

4.2.3 The kernel on the cylinder

We have now to calculate the strong coupling expansion for the basic building block of the partition function (94), namely the QCD2 kernel on the cylinder $\mathcal{K}_2(P, P^\dagger; 1/J)$. In the following we shall consider the more general case in which the holonomies g_1, g_2 at the boundaries of the cylinder are arbitrary.

Unlike the weak coupling regime, where we had to use the expression (82) for $\mathcal{K}_2(g_1, g_2^{-1}; 1/J)$ obtained by the Poisson summation formula, we use here the character expansion

$$\mathcal{K}_2(g_1, g_2^{-1}; 1/J) = \sum_R e^{-\frac{C_R}{2NJ}} \chi_R(g_1) \chi_R(g_2^{-1}). \quad (102)$$

which provides directly a strong coupling expansion of the free energy¹³. The expansion parameter is the following function of the coupling J :

$$2 \exp \left(-\frac{1}{2J} \right). \quad (103)$$

¹³This is the free energy of the QCD2 on the cylinder, of course, and is just an ingredient of the free energy for the effective model of Polyakov loops that we are managing to build up.

Table II: Representations contributing to the strong coupling expansion of the free energy, up to the second order in $e^{-\frac{1}{J}}$. The fundamental, symmetric and anti-symmetric rank 2 tensor representations must be considered together with their conjugate representations.

representation	order	Casimir	Character
singlet	0	1	1
fundamental	1	$\frac{N^2-1}{N}$	$N\rho_1$
symm. rank 2 tensor	2	$\frac{2N^2+2N-4}{N}$	$(N^2\rho_1^2 + N\rho_2)/2$
anti-symm. rank 2 tensor	2	$\frac{2N^2-2N-4}{N}$	$(N^2\rho_1^2 - N\rho_2)/2$
adjoint	2	$2N$	$N^2 \rho_1 ^2 - 1$

which vanishes exponentially as J goes to zero. The free energy $F(g_1, g_2^{-1}; J)$ in the large N limit is defined by:

$$\mathcal{K}_2(g_1, g_2^{-1}; \frac{1}{J}) = e^{N^2 F(g_1, g_2^{-1}; J)} , \quad (104)$$

where, as usual, terms suppressed by powers of N in the exponent will be neglected. We have therefore

$$F(g_1, g_2^{-1}; J) = 2 e^{-1/2J} F_1^H(g_1, g_2^{-1}; J) + 4 e^{-1/J} F_2^H(g_1, g_2^{-1}; J) + \dots . \quad (105)$$

It is found that residual dependence on J in the individual terms is polynomial in $1/J$, and hence (105) is indeed a strong coupling expansion.

The coefficients $F_i^H(P, P^\dagger; J)$ of the strong coupling expansion of the free energy $F(P, P^\dagger; J)$ can be obtained in principle up to any order by using techniques which are summarized in Appendix A of [15]. They involve the large N expansion of the Casimirs C_r , and the expression of the characters, in the large N limit, in terms of the Fourier coefficients $\rho_k = \frac{1}{N} \text{Tr} P^k$ of the eigenvalue distribution (see also [45, 12]). In [15] this program was carried out up to the 4th order. The result is rather cumbersome and we shall not report it here, although we will use it in sec. 4.2.4 in order to derive the critical value of the coupling with the highest possible precision. We just reproduce here the calculation of the free energy eq. (105) up to the 2nd order, which illustrates all the basic points of the procedure, without being too involved. Let us define a representation r of $SU(N)$ to be of order l if the large N expansion of its Casimir is of the form $C_r = lN + O(1)$. It is clear from eq.s (102,104) that to work out an expression of the free energy in powers of $2e^{-\frac{1}{2J}}$ up to l^{th} order, we must take into account all the representations of order up to l . The relevant representations up to order two are given in Tab. II, together with the corresponding Casimirs and the large N expression for their characters.

By inserting the expressions in Tab. II into eq. (102) we obtain

$$\mathcal{K}_2 \sim 1 + 2N^2 |\rho_1|^2 \left(1 + \frac{1}{2N^2 J} + \dots\right) e^{-\frac{1}{2J}} +$$

$$\begin{aligned}
& + 2 \cdot \frac{1}{4} |N^2 \rho_1^2 + N \rho_2|^2 \left(1 - \frac{1}{NJ} - \frac{2}{N^2 J} + \frac{1}{2N^2 J^2} + \dots\right) e^{-\frac{1}{J}} \\
& + 2 \cdot \frac{1}{4} |N^2 \rho_1^2 - N \rho_2|^2 \left(1 + \frac{1}{NJ} - \frac{2}{N^2 J} + \frac{1}{2N^2 J^2} + \dots\right) e^{-\frac{1}{J}} \\
& + (N^2 |\rho_1|^2 - 1)^2 e^{-\frac{1}{J}} + O(e^{-\frac{3}{2J}}).
\end{aligned} \tag{106}$$

Eq. (106) can be exponentiated, as it is easy to check, as follows:

$$\mathcal{K}_2 \sim \exp \left\{ N^2 \left[2e^{-\frac{1}{2J}} x_1^2 + 4e^{-\frac{1}{J}} \left(-\frac{x_1^2}{2} + \frac{x_2^2}{4} - \frac{x_1^2 x_2 \cos(2\alpha_1 - \alpha_2)}{2J} + \frac{x_1^4}{8J^2} \right) + O\left(\frac{1}{N^2}\right) \right] \right\}, \tag{107}$$

where we have used the notation $\rho_k = x_k e^{i\alpha_k}$ introduced in the previous section. Eq. (107) provides the strong coupling expansion of the free energy $F(P, P^\dagger; J)$ up to the second order in $2e^{-\frac{1}{2J}}$. Notice that $F_k^H(P, P^\dagger; J)$, obtained from (107) for $k = 1, 2$, depends only on x_i and α_i with $i \leq k$; this property is general and valid at all orders in the expansion.

4.2.4 The deconfinement transition

By using eq.s (101) and (104,105) we can now express the large N limit of the partition function Z of eq. (94) as

$$\frac{1}{N^2} \log Z = \sum_{k=1}^{\infty} \left(d (2e^{-\frac{1}{2J}})^k F_k(x, \alpha) - \frac{x_k^2}{k} \right). \tag{108}$$

It is already obvious from (108) that, for small enough J , the free energy has a maximum for $x_k = 0$, that is for a uniform distribution of eigenvalues. The first order approximation of (108) can be obtained from (107) by neglecting the second order terms, and reads

$$\frac{1}{N^2} \log Z \approx (2e^{-\frac{1}{2J}} d - 1) x_1^2, \tag{109}$$

with all other x_k set to zero. The phase structure of (109) is very simple: for $J < \frac{1}{2 \log 2d}$ the maximum of the free energy occurs at $x_1 = 0$ and we are in the unbroken phase. Above the critical point $J = \frac{1}{2 \log 2d}$ we have instead $x_1 = 1/2$, which is the maximum value allowed by the positivity condition on $\rho(\theta)$.

A more accurate analysis of the phase diagram can be achieved by inserting in eq. (108) the available higher orders. As we are interested in determining the broken vacuum, we can set all α_n to zero, as discussed at the beginning of this section, and look at the maximum of the free energy regarded as a function of the x_n 's only.

In looking for the maximum, it is crucial to remain within the domain where $\rho(\theta)$ is positive or zero for any value of θ . This is far from trivial when we use the

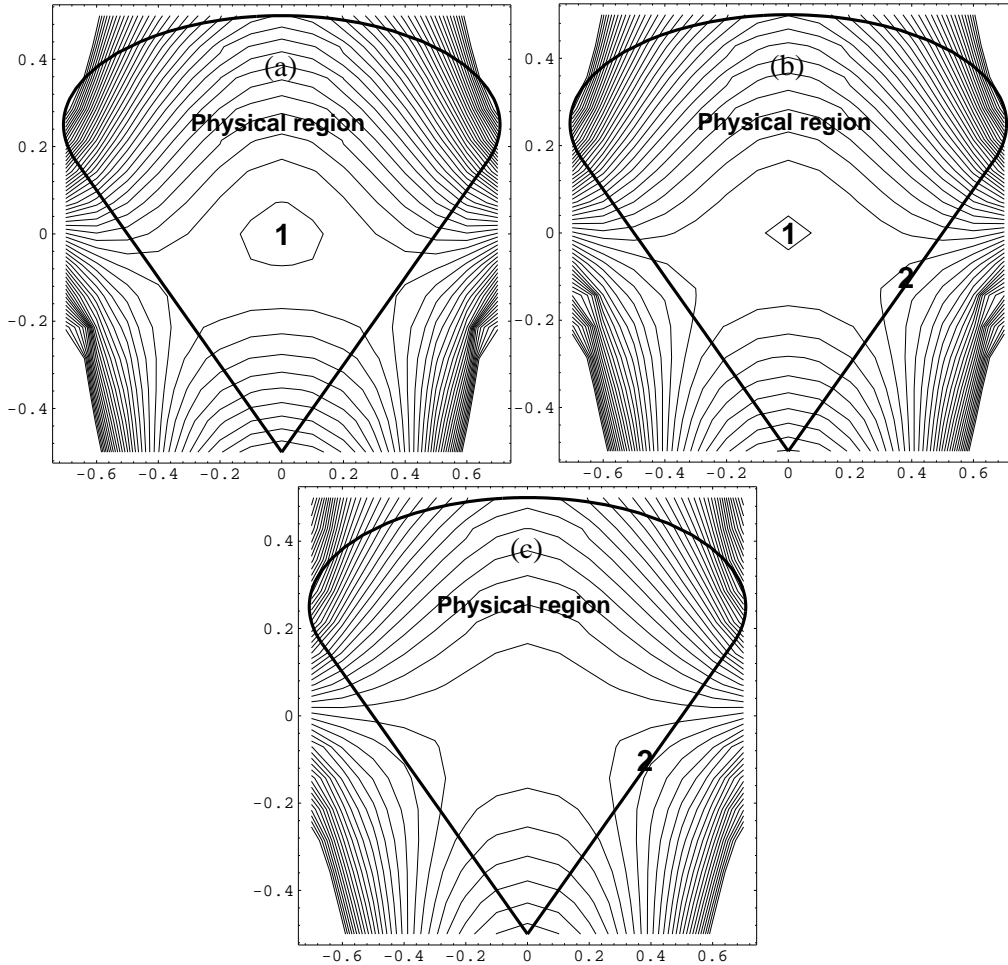


Fig. 6: Contour plots of the free energy for: (a), $J = 0.39$; (b), $J = 0.41$; (c), $J = 0.44$. The numbers **1** and **2** mark respectively the presence of the symmetric maximum ($x_1 = x_2 = 0$) and the “broken” one. The thick line encloses the “physical” region

Fourier coefficients x_k as dynamical variables. The equations for such a domain can be obtained in principle by requiring that, for some θ_0 ,

$$\rho(\theta_0) = \frac{d}{d\theta} \rho(\theta)|_{\theta=\theta_0} = 0 \quad (110)$$

and by eliminating θ_0 from the equations. The resulting equations for the x_n 's give the boundaries of the physical region.

Let us consider the second order approximation, whose corresponding free energy can be obtained by substituting (107) into (108). The contour plot of the free energy as a function of x_1 and x_2 at various values of the coupling J is shown in Fig. 6 for $d = 2$. The physical region in the (x_1, x_2) plane can be easily determined in this case, and it is represented by the region inside the thick line. The straight edge on the right is given by the equation $x_1 - x_2 = 1/2$ and corresponds to density

distributions vanishing at $\theta = \pi$, whereas the the straight edge on the opposite side corresponds to distributions vanishing at $\theta = 0$ ¹⁴. The plot at $J = 0.39$ clearly shows the maximum at $x_1 = x_2 = 0$: the system is in the unbroken phase dominated by a constant distribution of eigenvalues. In the next plot, at $J = 0.41$, a local maximum has appeared at the edge of the physical region, and it is becoming competitive with the unbroken maximum. Notice that there is a symmetry $x_1 \rightarrow -x_1$, so that a symmetric maximum appears on the other edge of the physical region. This symmetry is accidental, and it is removed when higher order terms are taken into account. In the last plot, at $J = 0.44$, the maximum at $x_1 = x_2 = 0$ has disappeared and the system is clearly in the broken phase. It is clear from this picture that there are three distinct regions of J : the first ranging from $J = 0$ to a $J_c^{(w.c.)}$ where only the symmetric maximum exist, the second from $J_c^{(w.c.)}$ to some value $J_c^{(s.c.)}$ where both the symmetric and the broken vacuum are present and the third for $J > J_c^{(s.c.)}$, where only the broken vacuum survives. The first order deconfinement transition occurs in the middle region at the critical J_c where the value of the free energy in correspondence of the two maxima is the same. The point $J_c^{(w.c.)}$ can likely be identified, when all orders are taken into account, with the critical coupling corresponding to the Douglas–Kazakov phase transition¹⁵, where the weak coupling solution becomes unstable. The instability of the symmetric solution will be investigated in the next subsection, where $J_c^{(s.c.)}$ is determined exactly, namely at all orders in the strong coupling expansion.

As more orders are taken into account the explicit calculation of the free energy as a function of the x_k 's becomes more and more involved and the determination of the physical region more complicated. In [15] the calculation is pushed up to the fourth order, where the free energy is a function of x_1, x_2, x_3 and x_4 and the boundaries of the physical region are given by fourth order algebraic equations, together with the hyperplanes $x_1 - x_2 + x_3 - x_4 = 1/2$ and $x_1 + x_2 + x_3 + x_4 = -1/2$.

The critical point can be determined numerically, and it is given for different dimensions by the values listed in Table III, where the values of the x_k 's corresponding to the broken vacuum at the critical point are also reported.

4.2.5 Instability of the symmetric vacuum

In the previous section, based on [15], we analysed the 1st order phase transition separating the confined and deconfined phase. It turns out that the two phases can coexist as meta-stable phases, at least for not too high values of d (see sec. 5.1). Indeed the weak coupling solution is still valid for couplings J lower than J_c , down to the value $J_c^{(w.c.)}$ determined in sec. 4.1.2 from the Douglas–Kazakov transition. In this section we shall show that it is possible to determine exactly the higher limit

¹⁴The curved section of the boundary is part of the ellipse of equation $8x_2^2 + x_1^2 - 4x_2 = 0$ and corresponds to eigenvalue distributions that vanish in two different points.

¹⁵This might not be the case, as discussed in sec. 5.1, for high values of d , the number of space dimensions.

Table III: Values of the critical coupling J_c at the fourth order in the strong coupling expansion of the heat kernel action. In the last four columns the corresponding values of x_i , ($i = 1 - 4$) are reported.

d	J	x_1	x_2	x_3	x_4
2	0.416	0.41	-0.13	0.03	0.07
3	0.282	0.45	-0.10	-0.01	0.05
4	0.238	0.50	-0.07	-0.05	0.02
100	0.094	0.64	0.07	-0.10	-0.03

$J_c^{(s.c.)}$ for the stability of the strong coupling symmetric vacuum [16, 46], i.e. the value for which the configuration $\rho = 1/2\pi$ ceases to be a local maximum; this value is found to be higher than J_c . We shall give here the main points of the calculation, a more detailed account of it can be found in [16, 46, 17].

The goal is achieved by calculating the spectrum of excitations around the strong coupling symmetric, translationally invariant vacuum $\rho(\theta, \vec{x}) = \frac{1}{2\pi}$. The instability appears when the lowest-lying excitation becomes massless.

As remarked several times, the configuration that dominates in the large N limit is the solution of the classical equations of motion for the model eq. (66). These equations can be derived from (66) by varying with respect to the eigenvalue distribution $\rho(\theta, \vec{x})$ of the Polyakov loop and by taking into account the large N expression of the integration measure given in (98). After taking the derivative with respect to θ , the resulting equations read:

$$- \wp \int_{-\pi}^{\pi} d\theta' \rho(\theta', \vec{x}) \cot \frac{\theta - \theta'}{2} = \frac{1}{N^2} \sum_{i=-d}^d \frac{\partial}{\partial \theta} \frac{\delta}{\delta \rho(\theta, \vec{x})} \log \mathcal{K}_2(P(\vec{x}), P^\dagger(\vec{x} + \hat{i}); 1/J), \quad (111)$$

where the left hand side comes from the integration measure. The dependence of the kernel $\mathcal{K}_2(P(\vec{x}), P^\dagger(\vec{x} + \hat{i}); 1/J)$ from $\rho(\theta, \vec{x})$ can be obtained in principle from the observation, discussed in sec. 4.1.2, that in the large N limit $\mathcal{K}_2(P(\vec{x}), P^\dagger(\vec{x} + \hat{i}); 1/J)$ is the transition amplitude, governed by the Das–Jevicki Hamiltonian (86), from an initial distribution $\rho(\theta, \vec{x})$ to a final distribution $\rho(\theta, \vec{x} + i)$ in a “time” $\frac{1}{J}$. Hence the logarithm of the kernel \mathcal{K}_2 is the classical action corresponding to the Das–Jevicki Hamiltonian, more precisely

$$\begin{aligned} & \frac{1}{N^2} \log \mathcal{K}_2(P(\vec{x}), P^\dagger(\vec{x} + \hat{i}); 1/J) \\ &= - \int_0^{\frac{1}{J}} dt \int d\theta \left[\Pi(\theta, t) \frac{\partial \rho(\theta, t)}{\partial t} - \frac{1}{2} \rho(\theta, t) \left\{ \left(\frac{\partial \Pi(\theta, t)}{\partial \theta} \right)^2 - \frac{\pi^2}{3} \rho^2(\theta, t) \right\} \right], \end{aligned}$$

where the field configurations are the *classical* trajectories, namely the solutions of

the Hopf equation (88) with the boundary conditions

$$\begin{aligned}\rho(\theta, 0) &= \rho(\theta, \vec{x}) , \\ \rho(\theta, \frac{1}{J}) &= \rho(\theta, \vec{x} + \hat{i}) .\end{aligned}\tag{112}$$

The explicit solution of the Hopf equation with arbitrary boundary condition is in general not known, but we are interested in small fluctuations around the symmetric vacuum configuration $\rho(\theta, t) = \frac{1}{2\pi}$, and we only need to retain in (112) quadratic terms in such fluctuations. In this approximation the Hopf equation becomes linear, and hence solvable. We shall skip here the details of the calculation, which can be found in [16]. Eq. (111) eventually reduces to a relation between the Fourier modes $\rho_n(\vec{x})$ of the eigenvalue distribution $\rho(\theta, \vec{x})$ on the sites of the lattice:

$$\sum_{i=1}^d \left(\rho_n(\vec{x} + \hat{i}) - 2 \left[\cosh \frac{n}{2J} - \frac{d-1}{d} \sinh \frac{n}{2J} \right] \rho_n(\vec{x}) + \rho_n(\vec{x} - \hat{i}) \right) = 0 ,\tag{113}$$

which is the free field equation for the scalar excitations $\rho_n(\vec{x})$ propagating on the lattice, provided their masses M_n are identified as follows:

$$M_n^2 = 2d \left(\cosh \frac{n}{2J} - 1 \right) - 2(d-1) \sinh \frac{n}{2J} .\tag{114}$$

The strong coupling vacuum becomes unstable when the first excitation becomes massless; setting $M_1^2(J_c^{(s.c.)}) = 0$ we obtain

$$\frac{1}{J_c^{(s.c.)}} = 2 \log(2d-1) .\tag{115}$$

The determination of the spectrum of excitations can be quite simply phrased also in the language of the previous sections 4.2.1-4.2.4. Indeed it corresponds to the determination of the free energy (108) *exactly* in J , but only up to quadratic terms in the x_n 's. In particular, the determination of the strong coupling vacuum instability $J_c^{(s.c.)}$ requires the determination of all the contributions to eq. (108) proportional to x_1^2 . This is within reach of the techniques developed in sec. (4.2.3), and the result is:

$$\begin{aligned}\frac{1}{N^2} \ln Z &\xrightarrow{x_1^2 \text{ terms}} \left[2d \left(e^{-\frac{1}{2J}} - e^{-\frac{1}{J}} + e^{-\frac{3}{2J}} - e^{-\frac{2}{J}} + \dots \right) d - 1 \right] x_1^2 \\ &= \left(\frac{2d e^{-\frac{1}{2J}}}{1 + e^{-\frac{1}{2J}}} - 1 \right) x_1^2 .\end{aligned}\tag{116}$$

By requiring the above expression to vanish we get $\exp(-1/2J_c^{(s.c.)}) = 1/(2d-1)$, namely eq. (115).

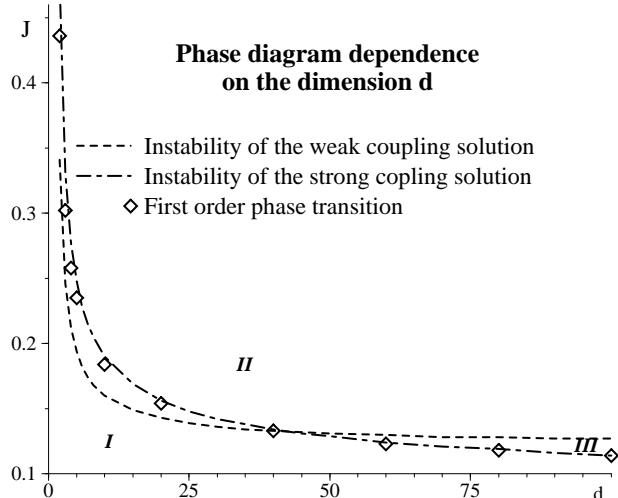


Fig. 7: We plot the point of instability $J_c^{(w.k.)}$ of the weak coupling solution, the point $J_c^{(s.k.)}$ where the strong coupling symmetric vacuum ceases to be a local maximum and the first-order transition point J_c in dependence of the dimensionality d of the lattice. It emerges that for $d \geq 40$ the weak coupling solution of eq. (81) loses its validity for higher coupling than those at which the symmetric vacuum becomes a maximum. This points to the existence of a new phase (III), beside the usual strongly coupled, confining one (I) and the weakly coupled, deconfined one described by the solution (81) (II). The phases II and III are separated by a third-order phase transition.

5 Extended phase diagrams

In the previous section we studied the phase diagram of the effective model for the Polyakov loop, as a function of the only existing parameter, namely the coupling J . In this section we consider some extensions of the model involving two parameters, and investigate the phase diagram in their plane, which reveals some new interesting features. The first example we shall consider is the same model studied in the previous section, but regarded as a function of J and of the number d of space dimensions. Secondly, following [17], we include the effect of external static sources in the adjoint representation (with coupling parameter λ) and consider the phase diagram in the (J, λ) plane. Finally we shall consider the effective action with the inclusion of an external “magnetic” field, as in the simplified effective action already studied in sec. 3.1.4, and describe how the phase diagram of Fig. 2 is modified as we go to higher orders in the strong coupling expansion.

5.1 Phase diagram in the (J, d) plane

The results obtained in the previous section, both in the weak and strong coupling regime, hold for any value of the space dimensionality d . So it is possible to plot both $J_c^{(w.c.)}$ and $J_c^{(s.c.)}$, marking respectively the DK phase transition and the instability of the symmetric vacuum, as a function of d . The plot is shown in Fig. 7.

For low values of d (up to $d \sim 40$) we have

$$J_c^{(w.c.)} < J_c < J_c^{(s.c.)} . \quad (117)$$

This is the situation already described in the previous section: in the interval between $J_c^{(w.c.)}$ and $J_c^{(s.c.)}$ both the weak coupling solution and the symmetric vacuum are present and a first order phase transition occurs somewhere in between. For $d > 40$ the situation is quite different. We have:

$$J_c < J_c^{(s.c.)} < J_c^{(w.c.)} . \quad (118)$$

Eq. (118) implies that if we approach the phase transition from the weak coupling (high J) region the semicircular solution becomes unstable *before* the appearing of the symmetric vacuum as a maximum of the effective action. This means a new phase, or even more than one new phase, is present for $d > 40$ in the region *III* between the two lines of Fig. 7. The features of this new, and presumably deconfined, phase(s) are not known, although a likely possibility is that the system goes from the weak coupling solution, where the density of eigenvalues vanish in an interval, to a distribution where it vanishes in one or in a discrete set of points. This phase is separated from the semicircular one by the third order transition due to the DK transition in QCD2. The existence of such intermediate phase(s) is also revealed by the circumstance that the radius of the semicircular distribution at the Douglas–Kazakov critical point goes to zero as d goes to infinity (see Table I), making the possibility of a sudden transition to a uniform distribution an extremely unlikely one.

5.2 Phase diagram in presence of adjoint quarks

Up to this point we have always been considering *pure* $SU(N)$ gauge theories. Recently in [17] an extension of the effective model considered in section 4 has been considered, by taking into account the effect of a gas of non-dynamical, static “quarks” (that is, a gas of “electric” non-abelian external sources) transforming in the adjoint representation of the gauge group. The phase diagram shows a rich structure, similar to that of the diagram in the J, d plane discussed in sec. 5.1 above.

Static sources couple only to the “electric” link matrices $V(\vec{x}, t)$ pointing in the time direction. The minimal introduction of such sources is therefore that of a quark–antiquark pair inserted both at the same spatial location \vec{x} . In presence of such a pair transforming in the adjoint representation, it is easy to see, by

using gauge invariance and the periodicity of the boundary conditions in the time direction, that the result of the integration in eq. (41) over the space-like links of the heat kernel action is multiplied by a factor of

$$\text{Tr}_{\text{adj}} P(\vec{x}) \equiv \left| \hat{P}(\vec{x}) \right|^2 - 1 . \quad (119)$$

The insertion of the sources is supposed to be governed by a fugacity $\lambda = e^{-\frac{\mu}{T}}$ (μ being the chemical potential). Therefore, in standard fashion, one inserts k such pairs at locations $\vec{x}_1, \dots, \vec{x}_k$ weighed with a factor of $\lambda^k/k!$, and sums over the positions and over k . The contribution of (119) is thus exponentiated and the effective model in the presence of a gas of adjoint static quarks becomes the following:

$$Z(\lambda) = \int \prod_{\vec{x}} DP(\vec{x}) \prod_{\vec{x}, i} \mathcal{K}_2(P(\vec{x}), P(\vec{x} + \hat{i}); 1/J) e^{\lambda \sum_{\vec{x}} (|\hat{P}(\vec{x})|^2 - 1)} , \quad (120)$$

which obviously reduces to the model (66) for $\lambda = 0$.

It is possible [17] to describe the phase diagram in the (J, λ) plane of the above model. To do so, in analogy to what we did in the case $\lambda = 0$, one determines the lines $J_c^{(\text{s.c.})}(\lambda)$ and $J_c^{(\text{w.c.})}(\lambda)$ at which the strong coupling and weak coupling solutions respectively lose their validity, and the line $J_c(\lambda)$ where the deconfinement transition takes place. It turns out that all these curves can be determined by the same techniques already exploited in the previous sections in the $\lambda = 0$ case. We will therefore presently discuss only the changes due to the new term, proportional to λ , in the model (120).

Let us consider first the instability of the strong coupling vacuum. It is possible to repeat the same discussion as in sec. 4.2.5; the extra λ -term gives obviously a contribution, namely

$$- 2\lambda \text{Im} \left(\rho_1(\vec{x}) e^{-i\theta} \right) , \quad (121)$$

to the eq.s of motion (111). It is clear from (121) that the new term affects uniquely the value of the mass of the 1st excitation, that becomes:

$$m_1^2 = 2d \left(\cosh \frac{1}{2J} - 1 \right) - 2(d - 1 + \lambda) \sinh \frac{1}{2J} \quad (122)$$

and vanishes for

$$\frac{1}{J_c^{(\text{s.c.})}(\lambda)} = 2 \log \frac{2d - 1 + \lambda d}{1 - \lambda d} . \quad (123)$$

It is possible determine numerically the value of J at which the first order deconfinement transition occurs at fixed values of λ , by adding a term $d \lambda (x_1^2 - 1)$ to the free energy and using the method described in sec. 4.2.4. The actual values obtained in the case $d = 2$ are reported in Fig. 8. In any case, the curve of instability $J_c^{(\text{s.c.})}$ of the strong coupling vacuum represents an upper bound for the curve $J_c(\lambda)$ of deconfinement transition, as it is indicated in Fig. 8.

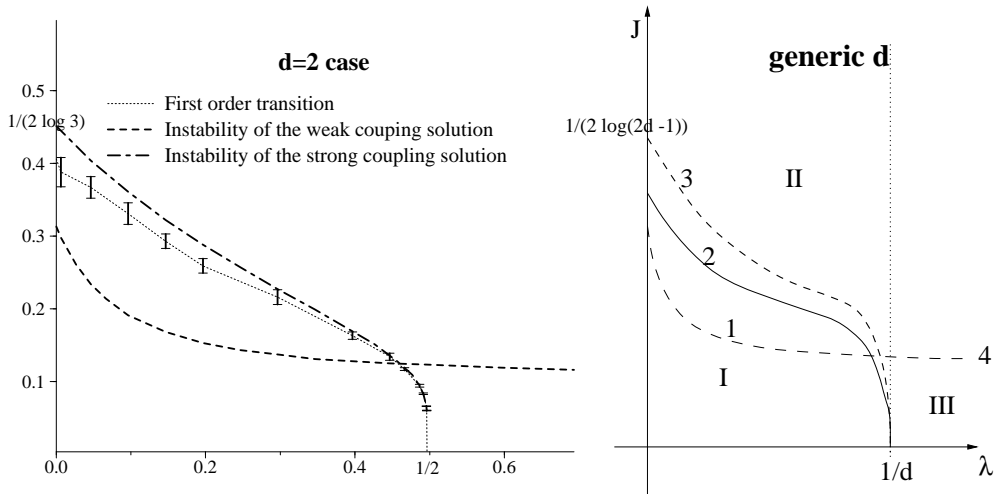


Fig. 8: The phase diagram in the λ, J plane for generic dimension d is determined by the line $J = J_c^{(w.k.)}(\lambda)$ where the weak coupling solution becomes unstable (1); the line $J = J_c^{(s.k.)}(\lambda)$ where the strong coupling symmetric vacuum turns into a minimum (3); the line of 1st order transition $J = J_c(\lambda)$ where the symmetric vacuum ceases to be energetically favourable (2). As remarked in Ref. [17], besides the strong coupling confining phase (I) and the weak coupling, deconfined one (II), a new region appears (III), separated from (II) by a line of 3rd-order transition (4). In the specific case $d = 2$ the actual numerical results for the 1st order transition, obtained as discussed in the text, are reported. The error bars estimate the uncertainty in the numerical procedure utilized for the calculation.

In the weak coupling regime, the model (120) can again be approximated by a Kazakov–Migdal model, as in the case (see sec. 4.1.1) when $\lambda = 0$. Indeed if we expand the additional term $\lambda(|\text{Tr}P|^2 - 1)$ up to the quadratic order in the invariant angles θ_i of the Polyakov loop we find that eq.(73) is replaced by:

$$\int \prod_i d\theta_i [\Delta^2(\theta)]^{(1-d)} e^{-N[dJ - \frac{d-1}{12} + \lambda] \sum_i \theta_i^2} \left[\sum_P (-1)^{\sigma(P)} e^{NJ\theta_i \theta_{P(i)}} \right]^d. \quad (124)$$

Eq. (124) is a quadratic Kazakov–Migdal model, with λ -dependent mass

$$m^2(\lambda) = 2d + \left(2\lambda - \frac{d-1}{6} \right) \frac{1}{J}. \quad (125)$$

The Gross solution of this model, that describes the vacuum in the weak coupling, deconfined phase, is a semicircular Wigner distribution with radius $r(\lambda)$ determined by eq. (81), but with m replaced with $m(\lambda)$. As described in sec. 4.1.2, the solution becomes unstable, as a consequence of the Douglas–Kazakov 3rd order transition in

QCD2, at the value $J_c^{(w.c)}(\lambda)$ that satisfies the equation

$$\left(\frac{1}{J(\lambda)}\right)^2 = \pi^4 - \pi^2 r^2(\lambda) . \quad (126)$$

The resulting curve is plotted in the case $d = 2$ and sketched in the generic d case in Fig. 8. In analogy with the (J, d) plane, the (J, λ) phase diagram reveals the presence of a region where neither the symmetric vacuum nor the weak coupling solution are stable and one or more new phases must exist. As a matter of fact, for $\lambda > \frac{1}{d}$, the symmetric vacuum is unstable for any value of J .

5.3 Phase diagram in presence of a “magnetic field”

In sec. 3.1.4 we discussed a simplified exactly solvable model for the Polyakov loop, obtained essentially by truncating the strong coupling expansion to the first order and adding to the free energy a “magnetic field” term $hN \sum_{\vec{x}} [\text{Tr}(P(\vec{x}) + P^\dagger(\vec{x}))]$. The phase diagram of this model consists of a line of 3rd order phase transition ending into a point of first order phase transition (see Fig. 2). The inclusion of the “magnetic field” to the full “zeroth order approximation” (41) can be studied in both the weak and strong coupling regime.

In the strong coupling expansion it corresponds to adding a term $-2hx_1$ to the free energy, namely to the l.h.s. of eq. (108). The resulting action can be investigated, in the spirit of sec. 4.2.4, by truncating for instance the expansion at the second order (instead of the first order as in the simplified model of 3.1.4). With reference to Fig. 6 of sec. 4.2.4, we find that the inclusion of the magnetic term shifts the central maximum towards the edge of the physical region even for $J = 0$: the symmetry is explicitly broken by the magnetic term. We can distinguish three different cases:

$$a) \ h < \sim 0.15 , \quad b) \ \sim 0.15 < h < 1/2 , \quad c) \ h > 1/2 .$$

For $h < \sim 0.15$ the phase transition is described by the same pattern shown in Fig. 6, except that the maximum “1” is not anymore located at the origin and it actually moves towards the edge of the physical region as J increases. In the simplified model corresponding to the first order truncation of the strong coupling expansion, this interval ($h < \sim 0.15$) shrinks to the point $h = 0$ where the first order phase transition occurs. For $\sim 0.15 < h < 1/2$ the maximum “1” reaches the edge of the physical region as J increases *before* maximum “2” develops. The transition is therefore of the third order. This interval corresponds to the line of third order phase transition in the simplified model. Finally, for $h > 1/2$ “1” is already outside the physical region at $J = 0$ and, as in the simplified model, there is no obvious phase transition at this order of the strong coupling expansion¹⁶.

¹⁶However, due to the non analyticity of the boundary of the physical region, a phase transition

In the weak coupling limit, one can reduce the model with magnetic term to a Kazakov–Migdal model, by expanding it in powers of θ_i up to quadratic terms. The result is identical to eq. (124) with λ replaced by h . This shows that even for $h > 1/2$ a phase transition of the Douglas–Kazakov type occurs, separating the weak coupling solution from some unknown phase.

6 Results in the framework of the Wilson Action

6.1 Eguchi–Kawai Model

In sec. 3.2.2 a complete dimensional reduction was obtained by using techniques of the type used in the derivation of the twisted Eguchi–Kawai model. The resulting action (60) has $N_t = 1$ and it is completely equivalent in the large N limit to the original unreduced action. By inserting the correct value of m determined in eq. (64) into eq. (60) we obtain the following expression for the dimensionally reduced effective action:

$$S_{\text{red}} = \beta_t N \sum_{\vec{x}} \sum_{i=1}^d \text{Re} e^{i\frac{2\pi}{N_t}} \text{Tr} [U_i(\vec{x}) V(\vec{x} + \hat{i}) U_i^\dagger(\vec{x}) V^\dagger(\vec{x})] + \beta_s N \sum_{\vec{x}} \sum_{i>j} \text{Re} \text{Tr} [U_i(\vec{x}) U_j(\vec{x} + \hat{i}) U_i^\dagger(\vec{x} + \hat{j}) U_j^\dagger(\vec{x})] . \quad (127)$$

In spite of the complete dimensional reduction, this model is still too complex to be solved exactly, and a solution has been obtained so far only in zeroth order approximation ($\beta_s = 0$) [18]. However, even within this approximation, the solution will retain a non trivial dependence from N_t , resulting from the exact dimensional reduction. In this section we shall derive and discuss such solution.

In order to obtain from (127) a solvable matrix model we assume that an \vec{x} independent master field dominates the functional integral so that the field variables in (60) can be replaced by constants. Then, setting $\beta_s = 0$, we get the following partition function:

$$Z = \int DV \int \prod_{i=1}^d DU_i e^{\beta_t N \text{Re} e^{i\frac{2\pi}{N_t}} \sum_{i=1}^d \text{Tr} (V U_i V^\dagger U_i^\dagger)} . \quad (128)$$

For $d = 3$, and more generally for odd values of d (that is even space-time dimensions), this result coincides with the one we would have obtained from a hot twisted Eguchi–Kawai model; the derivation shown here however holds for any d . The integrations over the unitary matrices U_i in eq. (128) are all independent and

occurs if the maximum moves from the straight to the curved section of the boundary. Numerical calculations indicate that this is indeed the case. Besides, the weak coupling analysis, as mentioned below, shows that a DK phase transition is bound to occur even for $h > 1/2$.

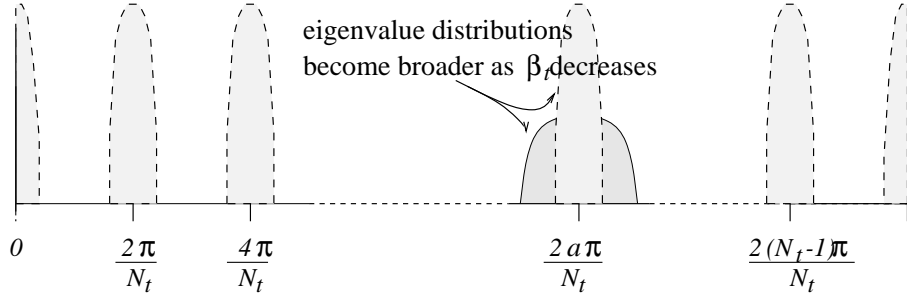


Fig. 9: The weak coupling solution in the large $\frac{N}{N_t}$ consists of N_t distributions, centered at the multiples of $\frac{2\pi}{N_t}$. The width of the distributions grows as β_t decreases, until finally an instability is attained at a certain critical value $\beta_{t,c}$.

the partition function can then be written as

$$\begin{aligned}
Z &= \int DV \left[\int DU e^{\beta_t N \text{Re} e^{i\frac{2\pi}{N_t} \text{Tr}(VUV^\dagger U^\dagger)} \right]^d \\
&= \int \left(\prod_{i=1}^N d\theta_i \right) \mathcal{J}^2(\theta) \left[\int DU e^{\beta_t N \sum_{i,j} |U_{ij}|^2 \cos(\theta_i - \theta_j + \frac{2\pi}{L})} \right]^d, \quad (129)
\end{aligned}$$

where in the last line we have gauge-rotated the matrix U to diagonalize V :

$$V \rightarrow \text{diag}(e^{i\theta_0}, \dots, e^{i\theta_{N-1}}). \quad (130)$$

$\mathcal{J}(\theta)$ is the Haar measure of $SU(N)$ expressed in terms of integration over the eigenvalues $e^{i\theta_i}$ and defined in (69). We want to solve the model (129) in the weak coupling limit. In the extreme weak coupling region the functional integral is dominated by the vacuum configuration given in eq. (61), namely

$$V = Q_{N_t} \otimes \mathbf{1}_{N/N_t}. \quad (131)$$

In this configuration the eigenvalues of V are organised in N_t bunches¹⁷ each composed of $\frac{N}{N_t}$ identical values $e^{\frac{2\pi i a}{N_t}}$, $a = 1, \dots, N_t$. Quantum fluctuations around this vacuum configurations can be considered by parametrizing the invariant angles θ_i according to the equation:

$$\theta_i \equiv \theta_{a,\alpha} = \frac{2\pi a}{N_t} + \varphi_{a,\alpha}, \quad (132)$$

with $a = 1, \dots, N_t$, $\alpha = 1, \dots, \frac{N}{N_t}$. A solution of the model given in eq. (128) can be obtained through the following steps: *a*) insert eq. (132) into (129) and evaluate

¹⁷Notice however that the open Polyakov loop is given by $V^{N_t} = \mathbf{1}$.

the integral in DU by using a saddle point method; *b*) in the resulting effective action keep only the terms quadratic in the fluctuations $\varphi_{a,\alpha}$; *c*) solve the model obtained in this way, which turns out to be a Kazakov–Migdal model, and find the eigenvalue distribution. The details of the calculation can be found in Ref. [18]. Here we just remark about some of its most delicate points. As in the Itzykson–Zuber integral, the extrema of the integrand in the integral over DU are given by U coinciding with any element of the Weyl group, namely with any permutation of the eigenvalues θ_i . However in computing the integral with the saddle point method we only consider permutations that map each bunch of eigenvalues into the next one, namely:

$$P : \theta_{a,\alpha} \rightarrow \theta_{a+1,P_a(\alpha)} . \quad (133)$$

where $P_a(\alpha)$ corresponds to a permutation of the $\frac{N}{N_t}$ eigenvalues of the bunch at $\frac{2\pi a}{N_t}$. It is easy to see that the other permutations are exponentially depressed compared to the ones above, typically by a factor

$$\exp\left(\beta_t N \left(1 - \cos \frac{2\pi s}{N_t}\right)\right) \sim \exp\left(-\beta_t N \frac{2\pi^2 s^2}{N_t^2}\right) . \quad (134)$$

for each eigenvalue mapped from a bunch a into $a + 1 + s$. One can assume that neglecting these non perturbative contributions is justified in the weak coupling (large β_t) regime, while below a critical value of β_t one expects a phase transition to occur as a result of their condensation. As we shall see, this is indeed the case, and we shall be able to conclude that the non perturbative contributions corresponding to permutations different from the ones in (133) play in the present formulation the same role as the instantons in the Douglas–Kazakov phase transition discussed in the previous sections.

The result of the calculation, up to quadratic terms in $\varphi_{a,\alpha}$, is the following (see [18]):

$$\begin{aligned} & \int \left[\prod_{a\alpha} d\varphi_{a,\alpha} \right] \left[\prod_a \Delta^2(\varphi_a) \right]^{(1-d)} \exp\left\{ -\frac{N}{N_t} \left[\left(\beta_t N_t - \frac{N_t}{4}\right) d - \frac{d-1}{12} N_t^2 \right] \sum_{a,\alpha} \varphi_{a,\alpha}^2 \right\} \\ & \times \left(\sum_{\{P_a\}} (-1)^{\sigma(P_a)} \exp\left\{ \frac{N}{N_t} \left(\beta_t N_t - \frac{N_t}{4}\right) \sum_{a,\alpha} \varphi_{a,\alpha} \varphi_{a+1,P_a(\alpha)} \right\} \right)^d . \end{aligned} \quad (135)$$

The solution of this model can be obtained by assuming that the master field is translational invariant, namely invariant under the \mathbf{Z}_{N_t} symmetry of the vacuum . With this assumption, which is proved *a posteriori* to be correct in [18], all bunches of eigenvalues have the same distribution and we can set:

$$\varphi_{a,\alpha} \rightarrow \frac{\varphi_\alpha}{N_t} , \quad (136)$$

where φ_α is now of order 1 in the large N_t limit, whereas the fluctuations $\varphi_{a,\alpha}$ are of order $\frac{1}{N_t}$. Notice that since the Polyakov line is $P = V^{N_t}$, the angles φ_α are

the invariant angles ¹⁸ of P , and the corresponding eigenvalue distribution is the eigenvalue distribution of P . With the position (136) the partition function (135) reduces to the product of the partition functions of N_t identical models:

$$Z = \left[\int \prod_{\alpha=1}^n d\varphi_\alpha [\Delta^2(\varphi)]^{1-d} \exp\left\{-n\left[Jd - \frac{d-1}{12}\right] \sum_\alpha (\varphi_\alpha)^2\right\} \times \left(\sum_P (-1)^{\sigma(P)} \exp\left\{nJ \sum_\alpha \varphi_\alpha \varphi_{P\alpha}\right\} \right)^d \right]^{N_t}, \quad (137)$$

where we have defined $n = N/N_t$ and done the replacement

$$\frac{1}{N_t}(\beta_t - \frac{1}{4}) = J, \quad (138)$$

where J is just the “normalized” coupling of the heat kernel action (see eq. (44)). In fact, if we consider eq. (138) at $\rho = 1$ we find the linear rescaling

$$\beta(n_t) = n_t J + \frac{1}{4}, \quad (139)$$

in agreement with eq. (45). The comparison between eq.s (139) and (45) also determines the value of α_τ^0 . A more complete analysis of the ρ dependence however can be obtained by writing (138) with $N_t = \rho n_t$ and with $N_t = n_t$, and by eliminating J from the two equations. We find

$$\beta_t(\rho n_t) = \rho \left(\beta(n_t) - \frac{1}{4} \right) + \frac{1}{4}. \quad (140)$$

This equation gives the rescaling of the coupling constant induced by varying the asymmetry parameter ρ , and it should be compared with eq. (9), where $\beta_t \rightarrow \beta_t(\rho n_t)$ and $\beta \rightarrow \beta(n_t)$. From the rescaling (140) we can read off immediately the function $c_\tau(\rho)$:

$$c_\tau(\rho) = -\frac{1}{4} + \frac{1}{4\rho} + \dots. \quad (141)$$

This has to be compared with the expression (11) obtained by Karsch [20]:

$$c_\tau(\rho) = -0.2609 + \frac{1}{4\rho} + \dots. \quad (142)$$

The agreement between the two results is quite remarkable. In fact, although both calculations are based on evaluating one loop effects around the classical vacuum, this is done in the approach described here *after* a complete dimensional reduction and *neglecting* the effect of the space-like plaquettes, which were instead taken into account in Karsch’s calculation. This confirms a feature, that already emerged in

¹⁸Each eigenvalue φ_α has obviously a degeneracy N_t , as it appears in each bunch.

the case of SU(2) [26], namely that the corrections to $c_\tau(\rho)$ due to the space-like plaquettes are relatively small. As a consequence, and to the extent to which the space-like plaquettes can be safely neglected, the result (141) is independent from the number d of space dimensions, whereas Karsch's result was limited to $d = 3$. The agreement between (141) and (142) also represents a check of the consistency of the calculation, and in particular that only the fluctuations around the classical vacuum are relevant in the deconfined phase.

Apart from the replacement of N with n the expression in (137) raised to the N_t th power coincides with the Kazakov–Migdal partition function (73) obtained from the heat kernel action. Its solution is therefore given by the Wigner semicircular distribution of eigenvalues described in section 4.3, and the instability of the solution occurs exactly for the same value of J as described there. The complete agreement between the results of the heat kernel action and the ones obtained from the Wilson action in the present section confirms that for large n_t , where the coupling constants coincide, the two models are equivalent. This was expected, as discussed in sec. 3.1, and this result justifies *a posteriori* the assumption that the non perturbative contributions which have been neglected in the saddle point method, i.e. those involving permutations not of the form (132), are indeed irrelevant in the weak coupling phase. It is shown in [18] that these contributions can be put in one to one correspondence with the winding configurations (instantons) of the heat kernel model. So their condensation is expected to be responsible of the phase transition at the critical value of β_t , in the same way as the instantons are responsible for the Douglas–Kazakov phase transition.

In terms of the original invariant angles θ_i the eigenvalue distribution of our solution consists, as shown in Fig. 9, of a sequence of bunches, each made of $n = N/N_t$ eigenvalues, at intervals of $\frac{2\pi}{N_t}$. Each bunch is described by a Wigner semicircular distribution of radius $\frac{r}{N_t}$ with r^2 given by (81). Above the phase transition different bunches do not communicate with each other, except for the canonical shift of $\frac{2\pi}{N_t}$ due to the twist, and the partition function is just the one corresponding to a single bunch raised to the power N_t (see eq. (137)). The non-perturbative contributions, corresponding to interactions between other bunches, are suppressed by the exponential factor given in eq. (134).

The picture, discussed in sec 4.1.2, for the eigenvalues of the Polyakov loop in the heat kernel model is quite similar. Their distribution can be represented on an infinite line as a periodic distribution of period 2π , that before the phase transition consists of separate bunches of N eigenvalues. The contribution of a one-instanton configuration connecting a bunch to its neighbour is weighted by an exponential factor of $\exp((-2\pi^2\beta_t N/N_t))$, as can be seen from eq. (82), with $\mathcal{A} = 1/J \sim \frac{N_t}{\beta_t}$. This contribution coincides with the one-instanton contribution in the one-plaquette model, that is obtained setting $s = 1$ in eq. (134), if one takes into account that the number of eigenvalues in the latter case is $n = N/N_t$ instead of N . The contribution of the instantons to the classical action is then the same in the two models. This is a strong hint that they describe the same physics and that their condensation play

the same role in the phase transition.

6.2 Strong coupling expansion

Let us now consider the strong coupling expansion of the effective model for the Polyakov loops obtained from the Wilson action. We proceed by mimicking the treatment of the heat kernel case done in sec. 4.2, and we will just sketch the main points, referring to [15] for further details.

By assuming translational invariance, we can rewrite the Wilson partition function (2) as

$$Z_W = \int \prod_i d\theta_i \mathcal{J}^2(\theta) (\mathcal{I}(\theta, J_W))^d, \quad (143)$$

whence it is evident that the integral

$$\mathcal{I}(\theta, J_W) = \int DU \exp\left(N J_W \operatorname{Re} \operatorname{Tr} U e^{i\theta} U^\dagger e^{-i\theta}\right) \quad (144)$$

plays the same role as $\mathcal{K}_2(P, P^\dagger; 1/J)$ in the heat kernel case (compare with eq. (67)). It turns out [15] that the integral (143) admits a large N strong coupling expansion of the form:

$$\mathcal{I}(\theta, J) = \exp\left(N^2 \sum_{k=1}^{\infty} J_W^k \tilde{F}_k(x, \alpha)\right), \quad (145)$$

where the functions $\tilde{F}_k(x, \alpha)$ can be shown to depend only on x_i and α_i with $i \leq k$, and can be determined in principle by using Schwinger–Dyson equations. Correspondingly, the large N limit of the partition function Z_W becomes

$$\frac{1}{N^2} \ln Z_W = \sum_{k=1}^{\infty} \left(d J_W^k \tilde{F}_k(x, \alpha) - \frac{x_k^2}{k} \right). \quad (146)$$

This is exactly the same type of expansion occurring in the heat kernel case, see eq. (108). The expansion parameter is now the Wilson coupling J_W instead of the function $2 \exp[-1/(2J)]$ of the heat kernel coupling.

In particular, one finds that at the first order

$$\tilde{F}_1(x, \alpha) = x_1^2 = F_1(x, \alpha; J), \quad (147)$$

while at higher orders \tilde{F}_k and F_k begin to differ¹⁹.

At first order therefore the phase diagram resulting from the Wilson strong coupling expansion is *exactly* the same obtained in the heat kernel case (see eq. (109) and following text), expressed in terms of J_W instead of $2 \exp[-1/(2J)]$; thus the critical Wilson coupling is indeed given at this order by $J_{W,c} = 1/d$. Notice that

¹⁹The expression of $\tilde{F}_k(x, \alpha)$ up to the 4th order is given in [15], eq.s (65)–(68).

Table IV: Values of the critical coupling $J_{W,c}$ at the fourth order in the strong coupling expansion of the Wilson action. In the last four columns the corresponding values of x_i , ($i = 1 - 4$) are reported.

d	$J_{W,c}$	x_1	x_2	x_3	x_4
2	0.601	0.50	0.06	-0.03	-0.03
3	0.379	0.52	0.03	-0.03	-0.02
4	0.275	0.53	0.02	-0.03	-0.02
100	0.010	0.49	0.004	0.004	0.005

this is, as it was to be expected, the result that is found within the simple model reviewed in sec. 3.5, a model that was indeed obtained from the truncation to the first order of the Wilson action.

Of course the deconfinement transitions observed in the Wilson and the heat kernel regularization schemes correspond to the same physical phenomenon. From the above discussion it follows that this is the case if

$$J_W = 2 \exp\left(-\frac{1}{2J}\right) + \dots, \quad (148)$$

the extra terms in the r.h.s. being the effect of higher order corrections. This is just the relation between the two couplings given in (48) and valid in the strong coupling regime. This relation was derived in sec. 3.3 by comparing the strong coupling behaviour of the coefficients in the character expansions of the heat kernel and Wilson actions. The analysis of the deconfinement transition, by using the strong coupling expansion of the Wilson action, can be carried on in exactly the same way as in sec. 4.2.4, and the results up to the fourth order are summarized in Table IV. The results of Table IV all refer to $n_t = 1$. It is possible in principle to apply the same method to extract from the dimensionally reduced twisted action of eq. (128) with $\rho = 1$ a strong coupling expansion for any value of n_t . However, as the Polyakov loop coincides in (128) with $\text{Tr} V^{n_t}$, namely with x_{n_t} , higher and higher orders in the strong coupling expansion are needed to proceed to higher values of n_t . It is more convenient to use the values of Table IV as an input and use the scaling law (139) to extract the dependence from n_t .

7 Comparison with results from Montecarlo simulations

When comparing our results with those of Montecarlo simulations we must expect two kinds of systematic deviations.

- a) The first one is due to the large N approximation. This is however a rather small deviation. In fact, the lesson that we learn by looking at the Montecarlo simulations is that the large N limit results are reached for rather small values of N . For instance recent calculations on the glue-ball spectrum in (2+1) dimensions for low values of N have shown that already for $N \geq 3$ some mass ratios are well described with the leading term in the large N limit [47]. Thus we can consider our large N results as rather good approximations of the $N = 3$ case in which we are interested. At the same time rather large corrections are certainly present in the $N = 2$ case. Obviously, it would be highly desirable to have results from simulations for larger values of N , so as to study in detail the approach to the large N limit and test the analytic calculations reviewed here in a more stringent way. But this is not an easy task. Large N simulations have been performed only in the framework of the Eguchi–Kawai reduction scheme and are plagued by the presence of a bulk phase transition which shadows the deconfinement one.
- b) The second, more serious, problem is that, in order to solve the model, we had to neglect the space-like plaquettes in the original action. We have already discussed the consequences that this approximation has on the scaling laws in sec.s 3.1.3 and 6.1: only for $d = 2$ we find the correct scaling behaviour. The experience gained with the SU(2) [26] model however suggests that in the $n_t = 1$ case the corrections due to the space-like plaquettes are very small and that their effect is essentially negligible. Even if this case is not interesting from a phenomenological point of view, since $n_t = 1$ is too small to give informations on the continuum limit, it becomes very interesting as a test of our method. For this reason we shall devote sec. 7.1 to a discussion of this comparison. For larger values of n_t these corrections are not any more negligible and their importance increases as n_t increases. Notice that, as mentioned above, the corrections due to the inclusion of the space-like plaquettes have a different relevance in (2+1) and (3+1) dimensions. In (2+1) dimensions they do not affect the scaling behaviour, and in fact we shall be able to successfully compare not just the leading, but the next to leading term in the scaling law (139) with the results of Montecarlo simulations. On the contrary in (3+1) dimensions they completely change the scaling law. For this reason we shall discuss separately the (2+1) and the (3+1) dimensional cases in the following subsections.

7.1 $n_t = 1$ in (3+1) dimensions

In the $n_t = 1$ case we have only two results from Montecarlo simulations; they are however very interesting and carry a lot of information. The first one is for the SU(2) model [48]. It is very precise since it was obtained by using an original and very powerful non local algorithm (see [48] for the details). The value of

the critical temperature in our units is $J_{W,c} \equiv \beta_c/N^2 = 0.2185(1)$. The second results is for $N = 30$, hence in a situation in which the large N limit is a very good approximation. The critical coupling is $J_{W,c} \sim 0.38$. It was obtained in [49] within the framework of the Eguchi–Kawai reduction scheme. These results must be compared with what we have found in the case of the Wilson action. In this case our best estimate for the critical coupling in $(3 + 1)$ dimensions, obtained by means of the strong coupling expansion, is $J_{W,c} = 0.378$ as shown in Table IV. The agreement with the $N = 30$ value is indeed impressive. This is an interesting result and, compared with the naive results $J_{W,c} = 1/d = 0.333$ which one would obtain by using the simplified action of sec. 3.5, it shows the relevance of the higher order terms in the character expansion of our action. The rather large gap between the value of $J_{W,c}$ for $N = 2$ and $N = 30$ can be understood already at the level of the lowest order in the strong coupling expansion where, for $N = 2$ only, the reality of the fundamental representation leads to a critical coupling $J_{W,c} = \frac{1}{2d}$. It would be interesting to have the Montecarlo simulations for some intermediate value of N , to see how the large N limit is approached. Analytically this result could be obtained within the strong coupling expansion scheme developed for the large N limit. A different technique has been applied both for $N = 2$ [56] and for higher values of N [57] consisting in an improved mean field Bethe approximation that determines the asymptotic expansion of $J_{W,c}$ in powers of $1/d$. The results obtained so far can be summarized as follows:

$$\begin{aligned}
N = 2 & \quad J_{W,c} = \frac{1}{2d} + \frac{1}{4d^2} + \frac{13}{48d^3} + O\left(\frac{1}{d^4}\right), \\
N = 3 & \quad J_{W,c} = \frac{1}{d} - \frac{1}{4d^2} + O\left(\frac{1}{d^3}\right), \\
N > 3 & \quad J_{W,c} = \frac{1}{d} + \frac{1}{2d^2} + O\left(\frac{1}{d^3}\right).
\end{aligned} \tag{149}$$

Notice that for N larger than 3 the expansion is the same up to terms of order $\frac{1}{d^3}$, which means that already at $N = 4$ we are quite close to the large N limit. If one substitutes $d = 3$ in (149) keeping all known terms one obtains the values 0.2045, 0.306 and 0.389 for $N = 2$, $N = 3$ and $N > 3$ respectively. They significantly improve the lowest order results and they agree, within the approximation one would expect from the truncation, with the Montecarlo results.

7.2 2+1 dimensions

Very precise Montecarlo estimates of the deconfinement temperature in $(2+1)$ dimensions exist for the $N = 2$ and $N = 3$ models in the range $2 \leq n_t \leq 6$. These can be found in [50, 51, 52] and are reported in Tab. V. All these simulations were made with the standard Wilson action and at $\rho = 1$.

Looking at the data one can see that the expected linear dependence on n_t is very well fulfilled. This allows us to use the variable $\frac{T_c}{Ng^2} \equiv \frac{\beta_c}{n_t}$, which is the natural

one to take the continuum limit (see Tab. VI). Once the linear term is factored out we can see in Tab. VI a residual dependence on n_t which is due to the higher order terms of eq. (28). These corrections are so small that one can safely use a simple one parameter fit, keeping only the leading $O(1/\beta)$ correction, to extract reliable estimates for the continuum limit values of the critical temperature. These are reported in the last row of Tab. VI

As discussed in the previous sections, in the framework of the EK reduction scheme we can predict both the leading and sub-leading scaling behaviour. Remarkably enough, not only the functional form of these two terms, but also the *numerical estimates* of the correction that we find are in very good agreement with the simulations. They are reported in the last column of Tab. VI. They have been obtained by taking for $\beta_c(n_t = 1) = J_{W,c}$ our best strong coupling estimate given in Tab. IV and by using the scaling law (139) to extrapolate the result to arbitrary n_t . The result is:

$$\frac{T_c}{Ng^2} \equiv \frac{\beta_c(n_t)}{n_t} = 0.351 + \frac{1}{4n_t} . \quad (150)$$

This analytical prediction has to be compared with the following best fits, for the $N = 2$ and $N = 3$ cases, obtained from the Montecarlo data of Tab. VI by assuming a linear dependence of the critical coupling from $1/n_t$. Both fits have a high confidence level and give:

$$\begin{aligned} N = 2 & \quad \frac{\beta_c(n_t)}{n_t} = 0.380(3) + \frac{0.106(11)}{n_t} , \\ N = 3 & \quad \frac{\beta_c(n_t)}{n_t} = 0.366(2) + \frac{0.174(6)}{n_t} . \end{aligned} \quad (151)$$

The agreement of the analytic results (150) with the best fit (151) of the Montecarlo simulations is quite remarkable. In fact the trend shown in the $N = 2$ and $N = 3$ simulations is perfectly consistent with the theoretical large N limit not only in the leading term but also in the sub-leading one. Although it is premature to draw any conclusion, one can say that the results are at least consistent so far with the space-like plaquettes being negligible in $2 + 1$ dimensions as far as the determination of the deconfinement transition is concerned. Notice that in $d = 2$ there is no simulation for $n_t = 1$ to make a direct comparison as we did in the (3+1) case above. In [26, 53] however we obtained a rather reliable estimate of β_c in the SU(2) case. This value is reported in the first line of Tab. VI.

7.3 $n_t > 1$ in (3+1) dimensions

Very precise data on SU(2) and SU(3) in the range $n_t = 2 - 16$ can be found in [54]. Some results for higher values of N , obtained within the context of the EK model can be found in [55, 49]. We have collected in Tab. VII these results for the lowest values of n_t .

Table V: The critical coupling β_c as a function of the lattice size in the t direction, n_t , in the $(2+1)$ dimensional $SU(2)$ and $SU(3)$ LGT, taken from [50], [52] and [51].

n_t	$N = 2$	$N = 3$
2	~ 0.866	0.906(2)
3	~ 1.251	
4	1.630(8)	1.638(6)
6	2.388(10)	2.371(17)

Table VI: The critical temperature $\frac{T_c}{Ng^2} \equiv \frac{\beta_c}{n_t}$, in $(2 + 1)$ dimensions, as a function of n_t and N . In the first line of the $N = 2$ column is reported an analytic prediction obtained in [53] for $n_t = 1$, and in the last line the extrapolations to the continuum limit. The prediction of the analysis reviewed in this work is displayed in the last column.

n_t	$N = 2$	$N = 3$	$N = \infty$
1	~ 0.459		0.601
2	~ 0.433	0.4531(8)	0.476
3	~ 0.417		0.434
4	0.4075(19)	0.4094(14)	0.413
6	0.3979(16)	0.3952(27)	0.393
∞	0.380(3)	0.366(2)	0.351

Table VII: The critical coupling β_c/N^2 , in $(3 + 1)$ dimensions, as a function of n_t and N . In the last column our predictions, according to the scaling law eq.(46) and $\beta_c/N^2 = 0.378$ for $n_t = 1$.

n_t	$N = 2$	$N = 3$	$N = 24$	$N = 54$	$N = 81$	$N = 96$	$N = \infty$
2	0.4700(8)	~ 0.568	~ 0.70				0.506
3	0.5442(8)	0.6167(11)		~ 0.70			0.634
4	0.5746(2)	0.63250(2)				~ 0.70	0.762
5	0.5932(11)						0.890
6	0.6066(8)	0.65490(6)			0.705(5)		1.018

As mentioned above in this case we do not obtain in our approach the correct scaling law for the critical temperature as a function of n_t for which the inclusion of the space-like plaquette contribution is mandatory. Hence we can trust our results only for low values of n_t . We have already seen before that in the $n_t = 1$ case our

prediction is indeed successful, we shall now extend the comparison to higher values of n_t . To obtain our best estimate for the critical temperature in this case we use again the scaling relation eq. (139) and take our $n_t = 1$ value ($J_c = 0.378$) as input. These estimates are reported in the last column of Tab. VII.

A few comments are in order at this point:

- a) It is interesting to notice that the critical couplings for small values of n_t have a dependence on n_t which is not too different from ours. In fact, even if the scaling law eq. (139) is definitely different from the scaling behaviour eq. (33), for low values of n_t the Montecarlo estimates of the critical couplings are still far from the asymptotic scaling region and do not follow the scaling behaviour of eq. (33).
- b) At fixed n_t , as N increases also the critical temperature systematically increases, and our large N estimates seem to be the upper limit of this behaviour.
- c) For large values of N all the Montecarlo result cluster around the value ~ 0.70 . This is an artifact of the EK approximation. This value is due to the presence of a bulk transition which shadows the real deconfinement transition.

As we have seen, our results, obtained analytically in the large N limit, show a more than qualitative agreement with Montecarlo simulations performed on the full theory. We think that a careful analysis of higher order contributions in β_s , may allow in future further improvements in the analytic determination of the deconfinement critical temperature.

Acknowledgements

We would like to thank for discussions F. Gliozzi and particularly L. Magnea, with whom the work contained in Ref. [15] was carried out.

This work was partially supported by the European Commission TMR programme ERBFMRX-CT96-0045.

References

- [1] G. 't Hooft, Nucl. Phys. **B72** (1974) 461; E. Witten, Nuc. Phys. B 160 (1979) 57.
- [2] S. Coleman, in the Proceedings of the 17th Int. School on Subnuclear Physics, Erice 1979, ed A. Zichichi (1982).
- [3] S.M. Das, Rev. of Modern Physics **59** (1987) 235.
- [4] M. Campostrini, P. Rossi and E. Vicari, hep-th/9609003.
- [5] J.M. Drouffe and J.B. Zuber, Phys. Rep. **102**(1983) 1.
- [6] T. Eguchi and H. Kawai, Phys. Rev. Lett. **48** (1982) 1063.
- [7] M.L. Mehta, *Random Matrices*, Academic Press, San Diego, 1991.
- [8] E. Witten, Commun. Math. Phys. **141** (1991) 153; M. Blau and G. Thompson, Int. J. Mod. Phys. **A7** (1992) 3781.
- [9] B. Ye. Rusakov, Mod. Phys. Lett. **A5** (1990) 693
- [10] D.J. Gross and A. Matytsin, Nucl. Phys. **B429** (1994) 50.
- [11] D.J. Gross and A. Matytsin, Nucl. Phys. **B437** (1994) 541.
- [12] D.J. Gross, Nucl. Phys. **B400** (1993) 161; D. Gross and W. Taylor, Nucl. Phys. **B403** (1993) 395.
- [13] D.J. Gross and A. Migdal, Phys. Rev. Lett. 64 (1990) 127; Nucl. Phys. **B340** (1990) 333; E. Brézin and V.A. Kazakov, Phys. Lett. **B236** (1990) 144; M.R. Douglas and S.H. Shenker, Nucl. Phys. **B335** (1990) 635; see also J. Ambjørn, *Quantization of geometry*, lectures presented at the 1994 Les Houches Summer School 'Fluctuating Geometries in Statistical Mechanics and Field Theory' (hep-th/9411179).
- [14] V.A. Kazakov and A.A. Migdal, Nucl. Phys. **B397** (1993) 214.
- [15] M. Billó, M. Caselle, A. D'Adda, L. Magnea and S. Panzeri, Nucl. Phys. **B435** (1995) 172.
- [16] K. Zarembo, Mod. Phys. Lett. **A10** (1995) 677; Teor. i Mat. Fiz **104** (1995) 25.
- [17] G.W. Semenoff and K. Zarembo, SMI-96-4, hep-th/9606117.
- [18] M. Billó and A. D'Adda, hep-th/9607013, NORDITA 96/37P (1996), to appear on IJMPA.

- [19] D.J. Gross, Phys. Lett. **B293** (1992) 181.
- [20] F. Karsch, Nucl. Phys. **B205** (1982) 285.
- [21] B. Svetitsky and L. Yaffe, Nucl. Phys. **B210** (1982) 423.
- [22] S. Elitzur, R.B. Pearson and J. Shigemitsu, Phys. Rev. **D19** No 12 (1979) 3698.
- [23] N.D. Mermin, J. Math. Phys **8** (1967) 1061.; F.G. Wegner, J. Math. Phys. **12** (1971) 2259.
- [24] J.M. Kosterlitz and D.J. Thouless, J. Phys. **C6** (1973) 1181; V.L. Berezinskii, Zh. Eksp. Teor. Fiz. **59** (1970) 907.
- [25] A. Migdal, Sov. Phys. JETP **42** (1976) 413, 743; L.P. Kadanoff, Ann. Phys. (N.Y.) **100** (1976) 359; Rev. Mod. Phys. **49** (1977) 267.
- [26] M. Billó, M. Caselle, A. D’Adda and S. Panzeri, Nucl. Phys. **B472** (1996) 163.
- [27] M. Ogilvie Phys. Rev. Lett. **52** (1984) 1369.
- [28] J.M. Drouffe, J. Jurkiewicz and A. Krzywicki, Phys. Rev. **D29** (1984) 2982.
- [29] P.H. Damgaard and A. Patkos, Phys. Lett. **B172** (1986) 369.
- [30] A. Gocksch, F. Neri and P. Rossi, Phys. Lett. **B143** (1984) 207.
- [31] J. Polonyi and K. Szlachanyi, Phys. Lett. **B110** (1982) 395.
- [32] F. Green and F. Karsch, Nucl. Phys. **B238** (1984) 297.
- [33] P.H. Damgaard and M. Hasenbusch, Phys. Lett. **B331** (1994) 400.
- [34] D.J. Gross and E. Witten, Phys. Rev. **D21** (1980) 446.
- [35] M.R. Douglas and V.A. Kazakov, Phys. Lett. **B319** (1993) 219.
- [36] M. Caselle, A. D’Adda, L. Magnea and S. Panzeri, Nucl. Phys. **B416** (1994) 751.
- [37] I.I. Kogan, A. Morozov, G.W. Semenoff and N. Weiss, Nucl. Phys. **B395** (1993) 597.
- [38] Harish–Chandra, Am. I. Math. **79** (1957) 87; C. Itzykson and J.B. Zuber, J. Math. Phys. **21** (1980) 411; M.L. Mehta, Comm. Math. Phys **79** (1981) 327.
- [39] M. Caselle, A. D’Adda and S. Panzeri, Phys. Lett. **B302** (1993) 80.

- [40] M. Caselle, A. D'Adda, L. Magnea and S. Panzeri, [hep-th/9309107](#) , Proc. Trieste Summer School in High Energy Physics and Cosmology, World Scientific.
- [41] D. Altschuler and C. Itzykson, Ann. Hist. H. Poincaré, Phys. Théor. **54** (1991) 1.
- [42] S. Panzeri, Mod. Phys. Lett. **A8** (1993) 3201.
- [43] A. Matystsin, Nucl. Phys. **B411** (1994) 805.
- [44] S.R. Das and A. Jevicki, Mod. Phys. Lett. **A5** (1990) 1639.
- [45] I. Bars, J. Math. Phys. **21** (1980) 2678.
- [46] D.V. Boulatov, Mod. Phys. Lett. **A10** (1995) 2863.
- [47] M. Teper, communication at Lattice '96 (St. Louis), to appear in the Proceedings of the conference.
- [48] R. Ben-Av, H.G. Evertz, M. Marcu and S. Solomon, Phys. Rev. **D44** (1991) R2953.
- [49] F. Fabricius, O.Haan and F.R.Klinkhamer, Phys. Rev. **D30** (1984) 2227.
- [50] M.Teper, Phys. Lett. **B311** (1993) 223, Phys. Lett. **B313** (1993) 417.
- [51] J. Christensen, G. Thorleifsson, P.H. Damgaard and J.F. Wheeler, Nucl. Phys. **B374** (1992) 225.
- [52] J. Engels, F. Karsch, E. Laermann, C. Legeland, M. Lütgemeier, B. Petersson and T. Scheideler, [hep-lat/9608099](#).
- [53] M. Caselle, Talk given at the Enrico Fermi International School, Varenna, June 1995, DFTT 57/95, [hep-lat/9601009](#).
- [54] J. Fingberg, U. Heller and F. Karsch, Nucl. Phys. **B392** (1993) 493.
- [55] S. Das and J.B. Kogut, Phys. Rev. **D31** (1985) 2704.
- [56] L. Bertoglio, M. Billó, M. Caselle, A. D'Adda and S. Panzeri, in preparation.
- [57] L. Bertoglio, Tesi di Laurea - University of Torino (1995).